Supporting Information

For

Cycloaddition of CO_2 with epoxides into cyclic carbonates catalyzed by binary organocatalyst under mild conditions

Wen-Wang Yu, Xiang-Guang Meng*, Zi-Yu Gan, Wen Li, Yu-Lian Zhang, Jie Zhou

Key Laboratory of Green Chemistry and Technology Ministry of Education, College of Chemistry, Sichuan University, Chengdu 610064, P.R. China

*Corresponding Author.

Email address: mengxgchem@163.com

Table of Contents

Experimental section

1.1 Materials.

Epichlorohydrin, epibromohydrin, 1,2-Epoxyhexane, 3,4-epoxy-1-butene, 1,2-epoxy-5-hexene, 2-(oxiran-2-ylmethyl)isoindoline-1,3-dione, Isobutylene oxide, 2-(chloromethyl)-2-methyloxirane, glycidol, tert-butyl glycidyl ether, allyl glycidyl ether, glycidyl phenyl ether, benzyl glycidyl ether, furfuryl glycidyl ether, butyl glycidyl ether, 2-ethylhexyl glycidyl ether, glycidyl methacrylate, 1,2-epoxy-4-vinylcyclohexane, 3,4-epoxytetrahydrofuran, 3-boc-6-oxa-3-aza-bicyclo[3.1.0]hexane, trans-stilbene oxide, tetrabutylammonium formate, tetrabutylammonium triflate, 3-hydroxybenzylamine, 2-hydroxybenzylamine, 4-hydroxybenzylamine, propylene oxide, 1,2-epoxybutane, styrene oxide, 1,2-epoxydodecane, cyclopentene oxide, cyclohexene oxide, tetraethylammonium iodide, tetrabutylammonium iodide (n-Bu_4NI), tetramethylammonium iodide, tetraheptylammonium iodide, tetrabutylammonium hexafluorophosphate, tetrabutylammonium tetrafluoroborate, tetrabutylammonium bromide, tetrabutylammonium chloride, benzylamine, phenol were purchased from Aladdin Reagent. Ethylene glycol diglycidyl ether (epoxy value: 0.7 mol/100 g), 1,6-Hexanediol diglycidyl ether (epoxy value: 0.65-0.7 mol/100 g), neopentyl glycol diglycidyl ether (epoxy value: 0.68-0.75 mol/100 g), 1,4-Bis ((2,3-epoxypropoxy) methyl) cyclohexane (98%), resorcinol diglycidyl ether (epoxy value: 0.75-0.85 mol/100 g), 2,2-Bis(4-glycidyloxyphenyl)propane (epoxy value: 0.38-0.45 mol/100 g), Trimethylolpropane triglycidyl ether (epoxy value: 0.68-0.74 mol/100 g) were purchased from Adamas Reagent. All reagents were analytical grade and used without further purification. Distilled water was obtained from an in-house supply. Pure CO_2 (99.999%), N_2 (99.999%) and actual flue gas (14.5% CO_2, 2% H_2O, 1.5% O_2, 300 ppm CO, 207 ppm SO_x, 300 ppm NO_x and the other component was N_2) are supplied by Sichuan Chengdu Qiaoyuan Gas Company.

1.2 Instrumentation.

^1H NMR spectra were recorded at ambient temperature using a Bruker Avance III 400 spectrometer (^1H NMR 400 MHz, ^{13}C NMR 100 MHz). Fourier transform infrared (FT-IR) spectra were recorded on a Bruker Alpha spectrometer.

1.3 Experimental methods

1.3.1 General procedure for Cycloaddition reaction of CO_2 with terminal epoxides and glycerol derivatives.

Typically, epoxide (37.5 mmol), n-Bu_4NI (1.125 mmol) and 3-hydroxybenzylamine (1.125 mmol) were put into round-bottomed flask and stirred. After filling with carbon dioxide gas three times, the reaction bottle was connected to a balloon filled with carbon dioxide gas (1 atm) and sealed. After completing the reaction at 50 °C for 8 h, 20 μL of the reaction solution was taken out and dissolved in $CDCl_3$. The reaction solution was analyzed using nuclear magnetic resonance, and the conversion of epichlorohydrin and the selectivity of the carbonate were quantitatively calculated.

1.3.2 General procedure for Cycloaddition reaction of CO_2 with internal epoxides.

Typically, internal epoxide (37.5 mmol), n-Bu_4NI (1.125 mmol) and 3-hydroxybenzylamine (1.125 mmol) were put into stainless steel high-pressure autoclave equipped with stirring. The reactor was purged three times with CO_2, filled with 12 atm CO_2 and sealed. The reaction solution was heated to 110 °C and stirred at 300 r·min^{-1} for 18 h. After the reaction was completed, the high-pressure autoclave was cooled to room temperature and the remaining CO_2 is slowly discharged from the reactor. The other steps were the same as above.

1.3.3 General procedure for the cycloaddition reaction of 3a and CO_2 from simulated flue gas.

Typically, epichlorohydrin (37.5 mmol), n-Bu_4NI (1.125 mmol), and 3-hydroxybenzylamine (1.125 mmol) were mixed in round bottom flask. After blowing three times with different volume fractions of CO_2, the reaction bottle is connected to a balloon filled with different volume proportions of CO_2 and N_2 (1 atm) and sealed at room temperature. The reaction was carried out at 60 °C for 8 h. The other steps were the same as above.

1.3.4 General procedure for the cycloaddition reaction of 3a and CO_2 from actual flue gas.

Typically, epichlorohydrin (37.5 mmol), *n*-Bu_4NI (1.125 mmol), and 3-hydroxybenzylamine (1.125 mmol) are mixed in round bottom flask. After blowing three times with flue gas, the reaction bottle is connected to a balloon filled with flue gas (12648 cm^3) and sealed at 1 atm. The reaction was carried out at 60 °C for 10 h. The other reaction processes were similar to the above.

1.3.5 The molar amplification reaction of 3a in actual flue gas.

Typically, epichlorohydrin (375 mmol), *n*-Bu_4NI (11.25 mmol), and 3-hydroxybenzylamine (11.25 mmol) are mixed in round bottom flask. After blowing three times with flue gas, the reaction bottle is connected to a balloon filled with actual flue gas (63269 cm^3) and sealed at room temperature. The reaction was carried out at 70 °C and 1 atm for 14 h. The measurements of reactants and products were performed by NMR analysis.

1.3.6 The reusability of catalysts.

1,2-epoxybutane, **1a** and **2c** were mixed into round-bottomed flask, pursed three times with CO_2 gas, and connected to a balloon filled with CO_2 gas. Reaction was carried out at 50 °C and 1 atm CO_2 for 8 h. After the reaction was completed, 20 μL of reaction solution was extracted and dissolved in $CDCl_3$ for NMR spectroscopy analysis to obtain the yield of cyclic carbonate. The reaction solution was distilled under reduced pressure (76−79 °C, 2.0 mm Hg) to obtain the recovered binary organocatalyst. Since **1a** is dissolved in ethyl acetate and **2c** is insoluble in ethyl acetate, **2c** was obtained by heating and filtration after adding ethyl acetate and then the ethyl acetate solution was evaporated by rotation to get **1a**. Pure **1a** and **2c** were obtained by vacuum drying. The recovered catalyst was directly used for the next catalytic run and the procedure was repeated five times.

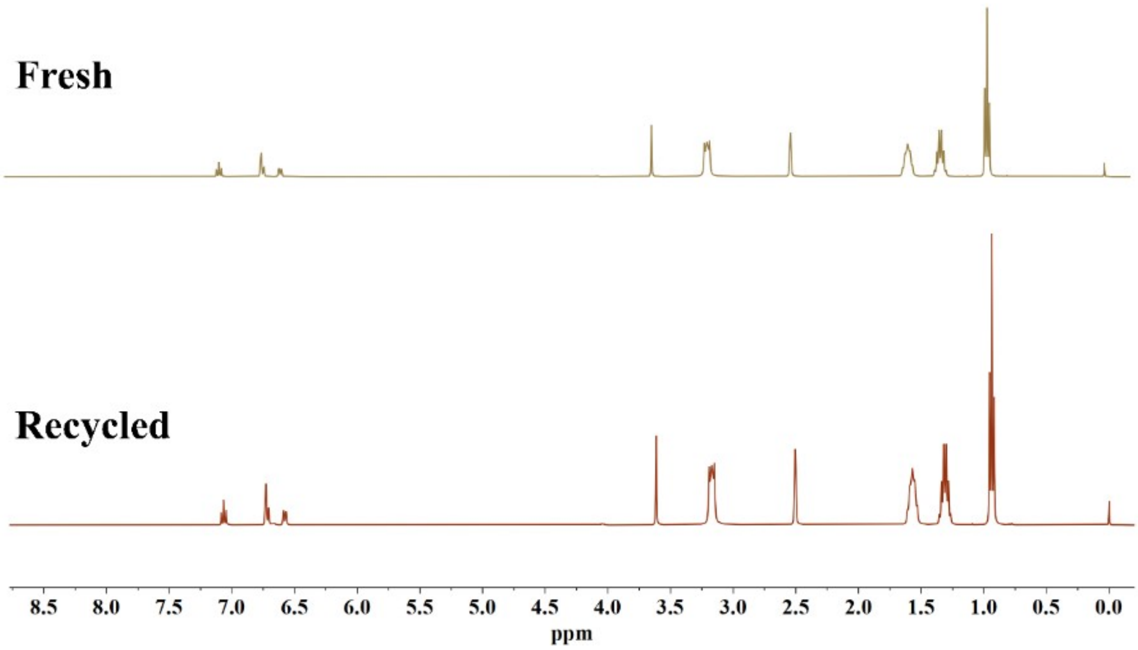

Fig. S1. ^{1}H NMR spectrum of fresh and recycled binary organocatalyst (400 MHz, DMSO, 298 K).

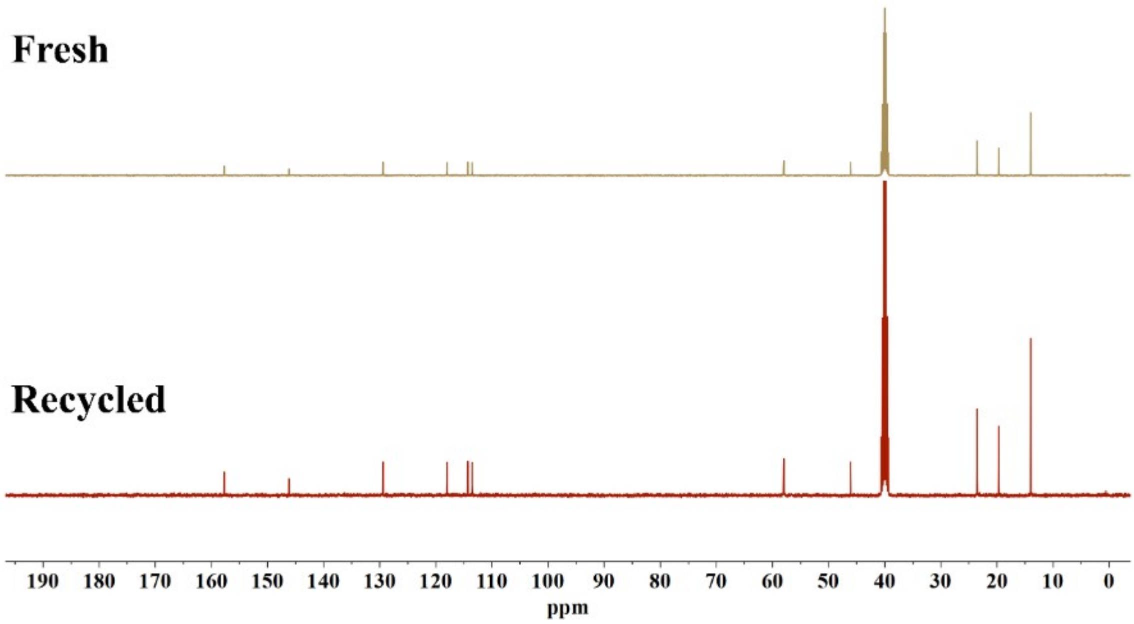

Fig. S2. ^{13}C NMR spectrum of fresh and recycled binary organocatalyst (126 MHz, DMSO, 298 K).

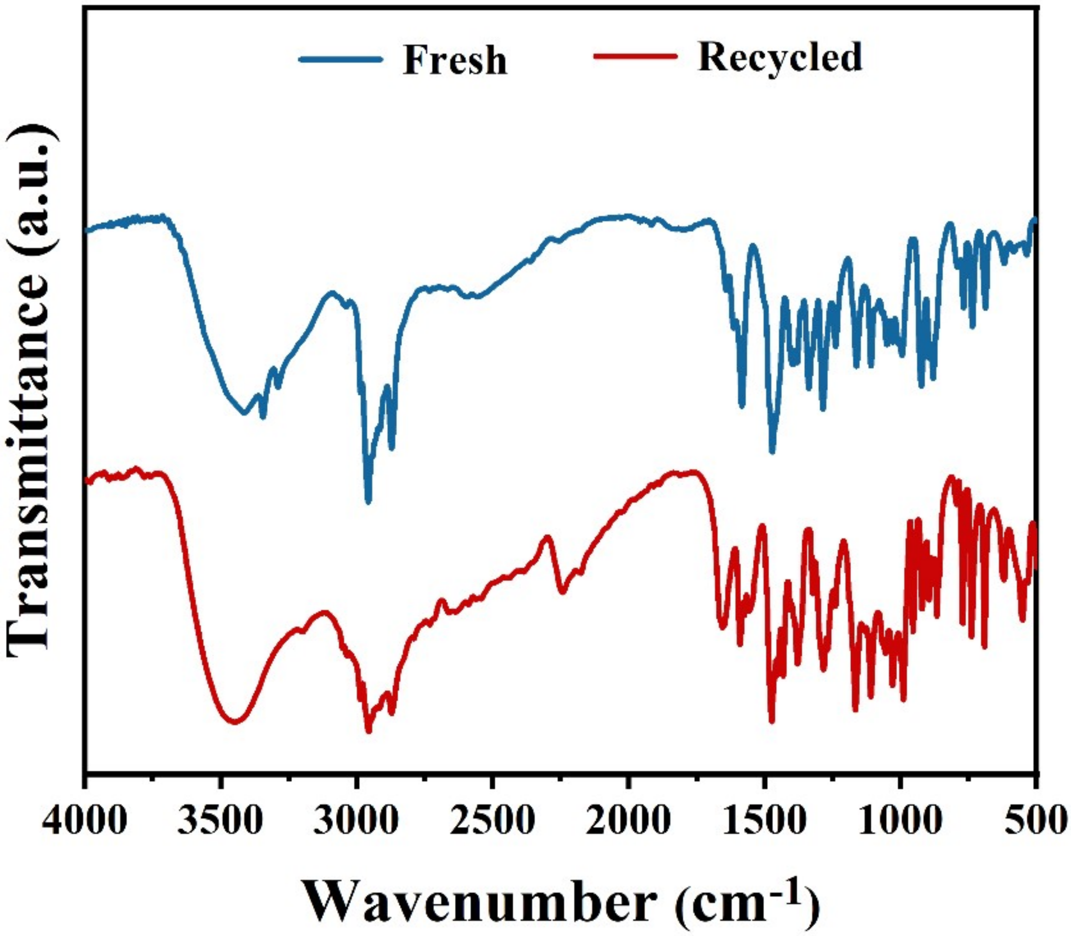

Fig. S3. FT-IR spectra of fresh and recycled binary organocatalyst.

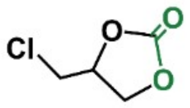

4a

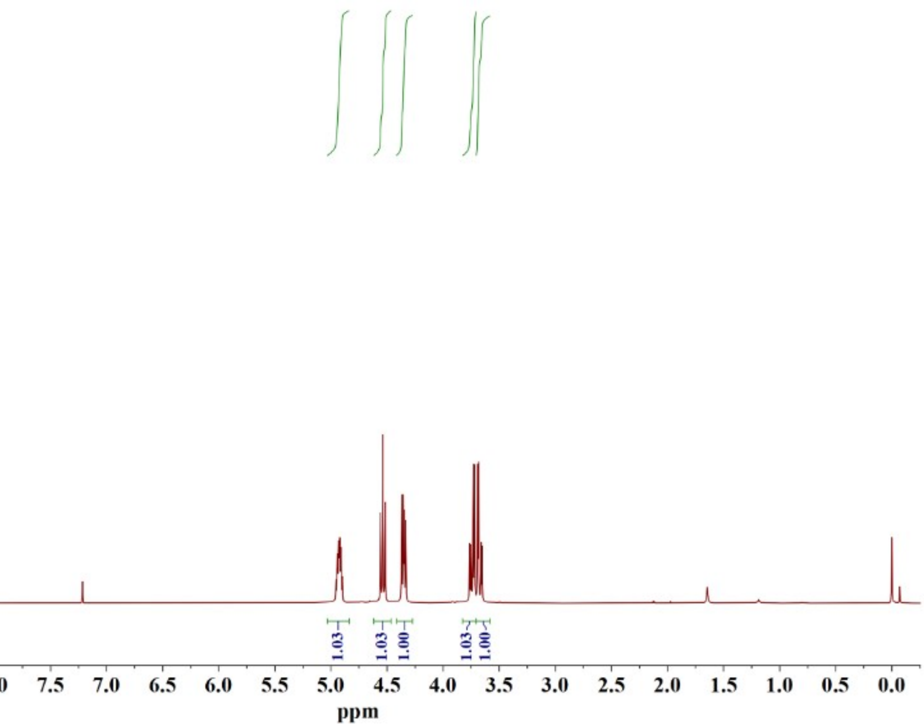

Fig. S4. ^{1}H NMR spectrum of **4a** (400 MHz, $CDCl_3$, 298 K).

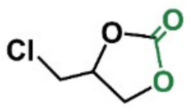

4a

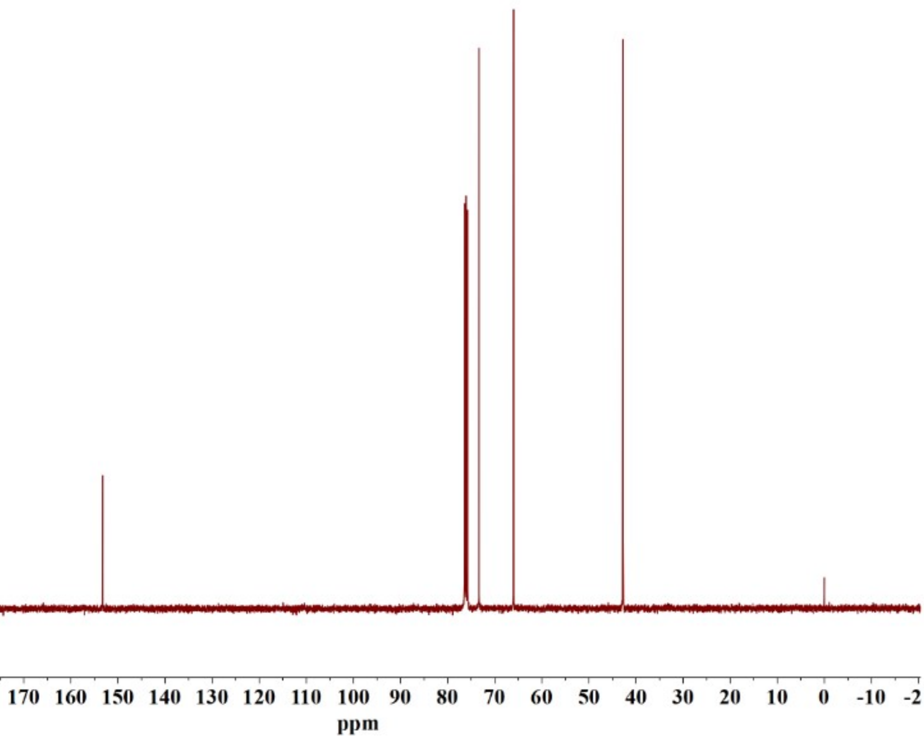

Fig. S5. ^{13}C NMR spectrum of **4a** (126 MHz, $CDCl_3$, 298 K).

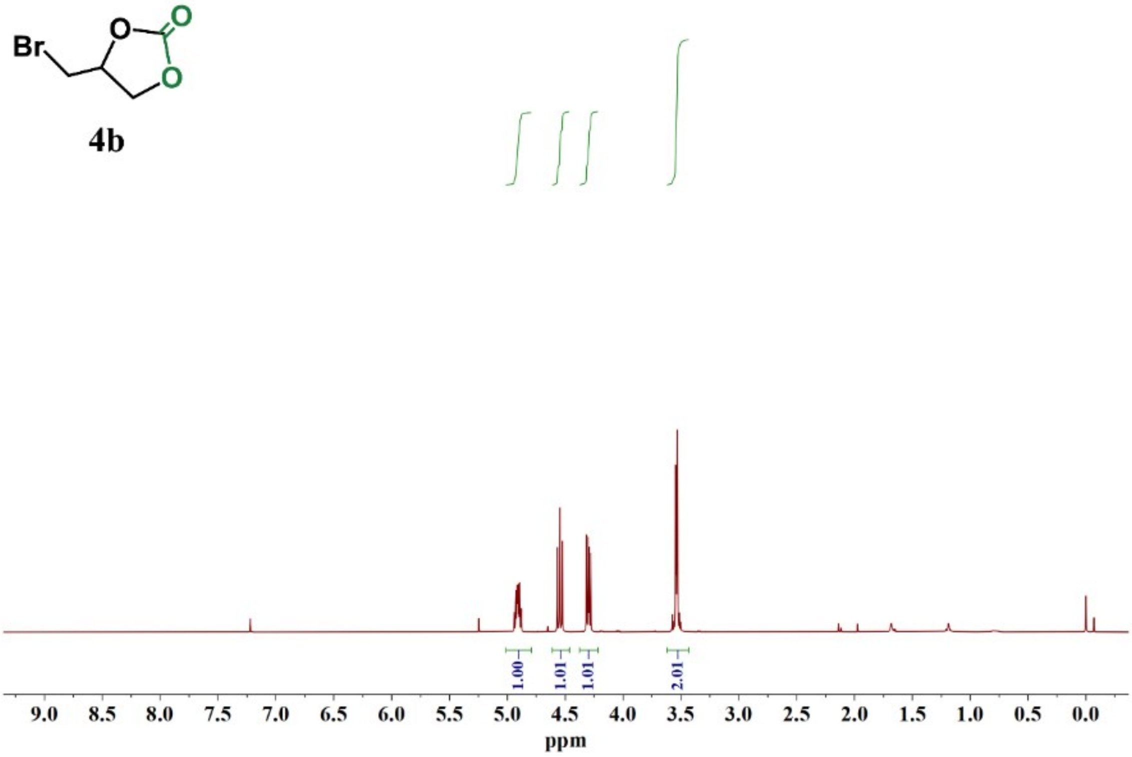

Fig. S6. ^{1}H NMR spectrum of **4b** (400 MHz, $CDCl_3$, 298 K).

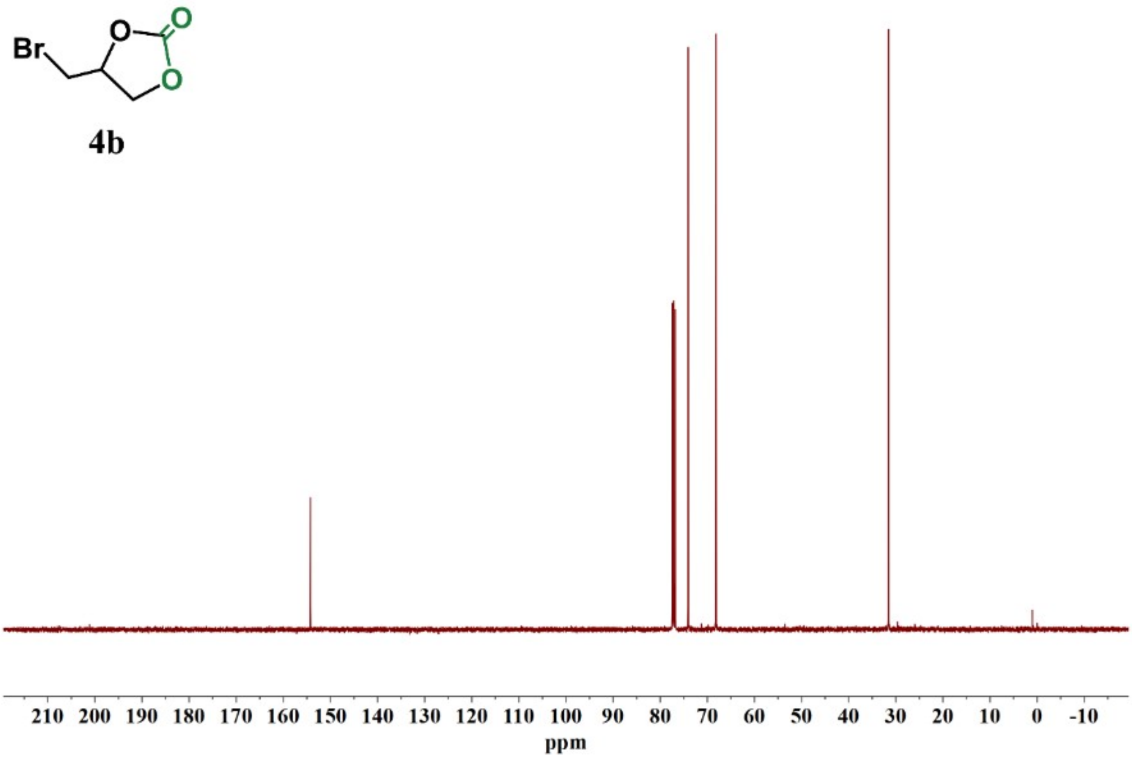

Fig. S7. ^{13}C NMR spectrum of **4b** (126 MHz, $CDCl_3$, 298 K).

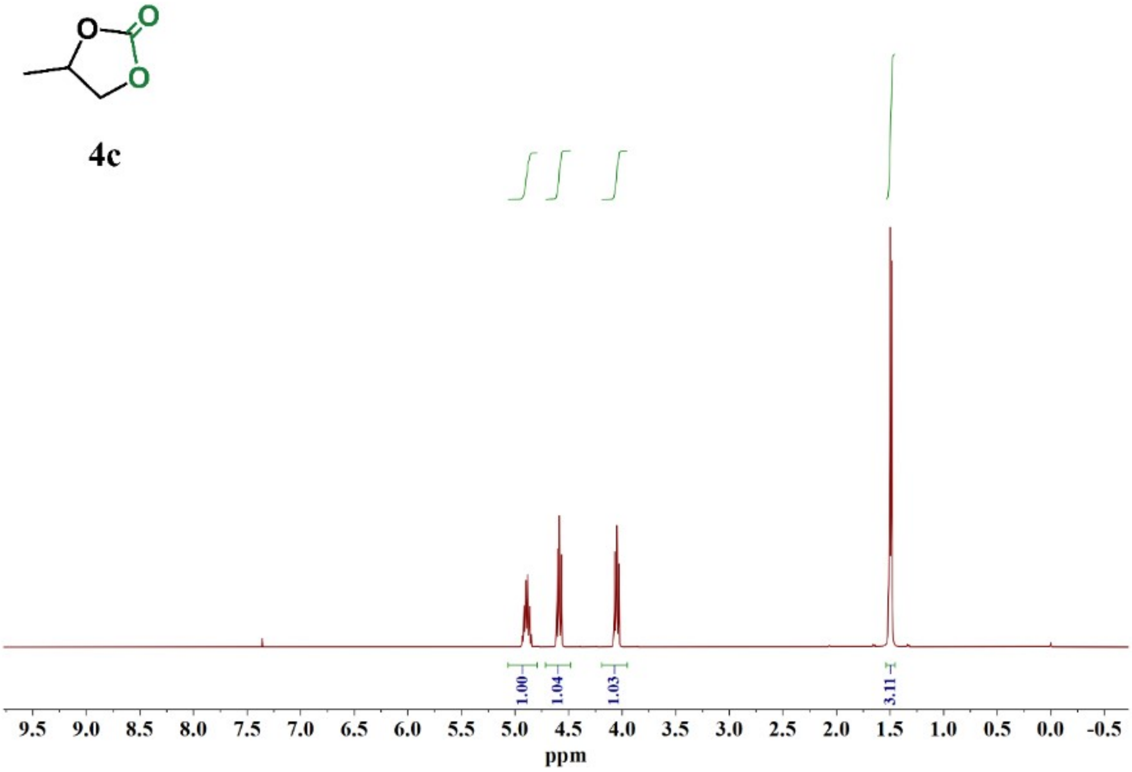

Fig. S8. ^{1}H NMR spectrum of **4c** (400 MHz, $CDCl_3$, 298 K).

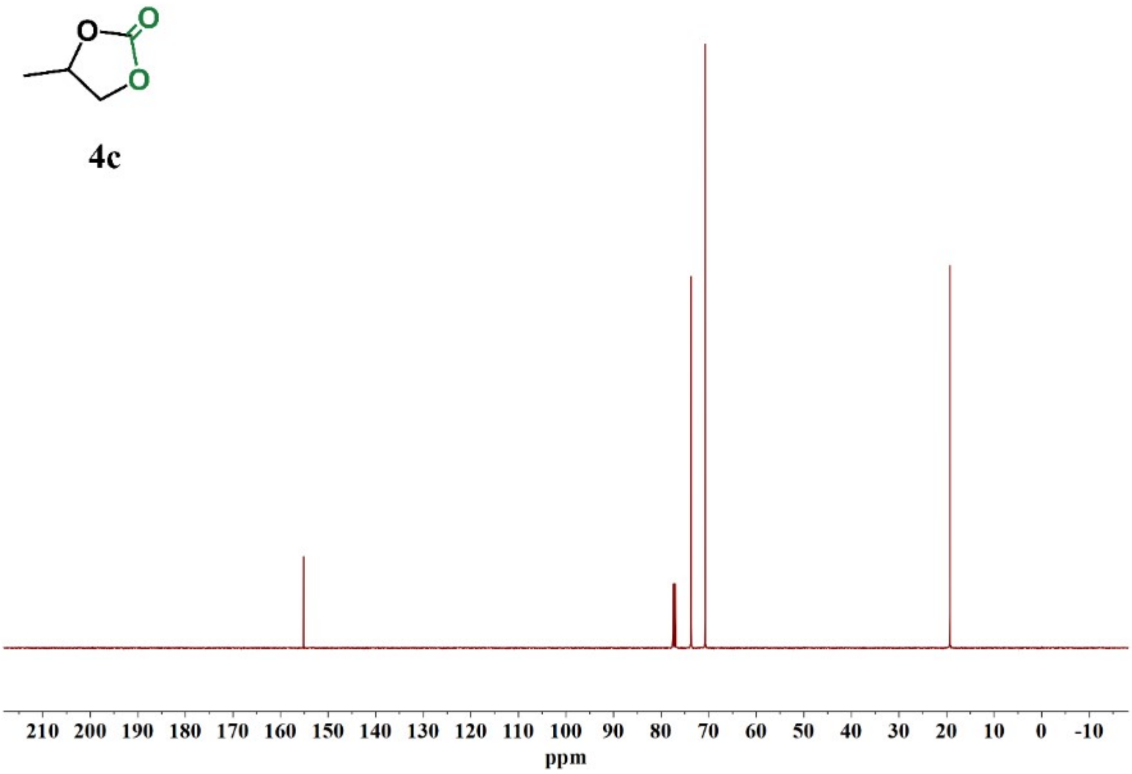

Fig. S9. ^{13}C NMR spectrum of **4c** (126 MHz, $CDCl_3$, 298 K).

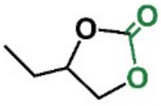

4d

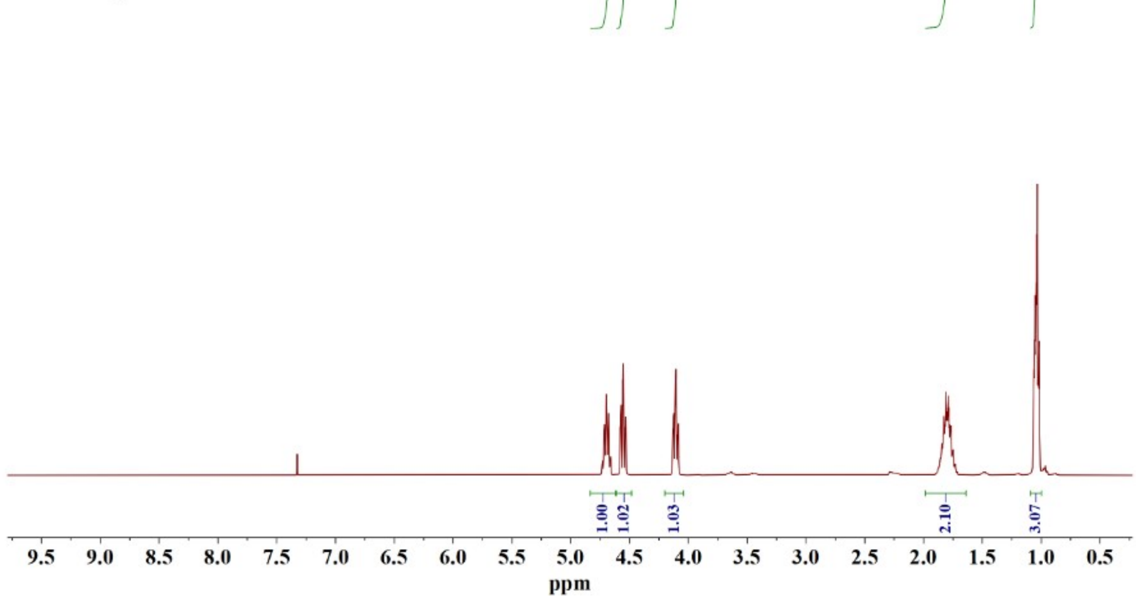

Fig. S10. ^{1}H NMR spectrum of **4d** (400 MHz, $CDCl_3$, 298 K).

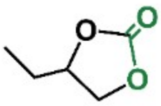

4d

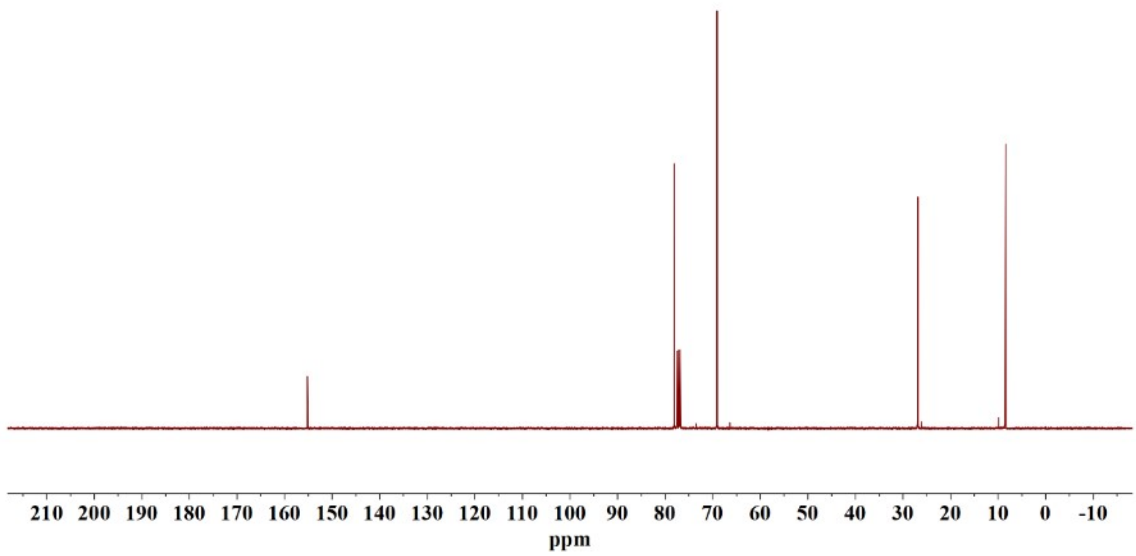

Fig. S11. ^{13}C NMR spectrum of **4d** (126 MHz, $CDCl_3$, 298 K).

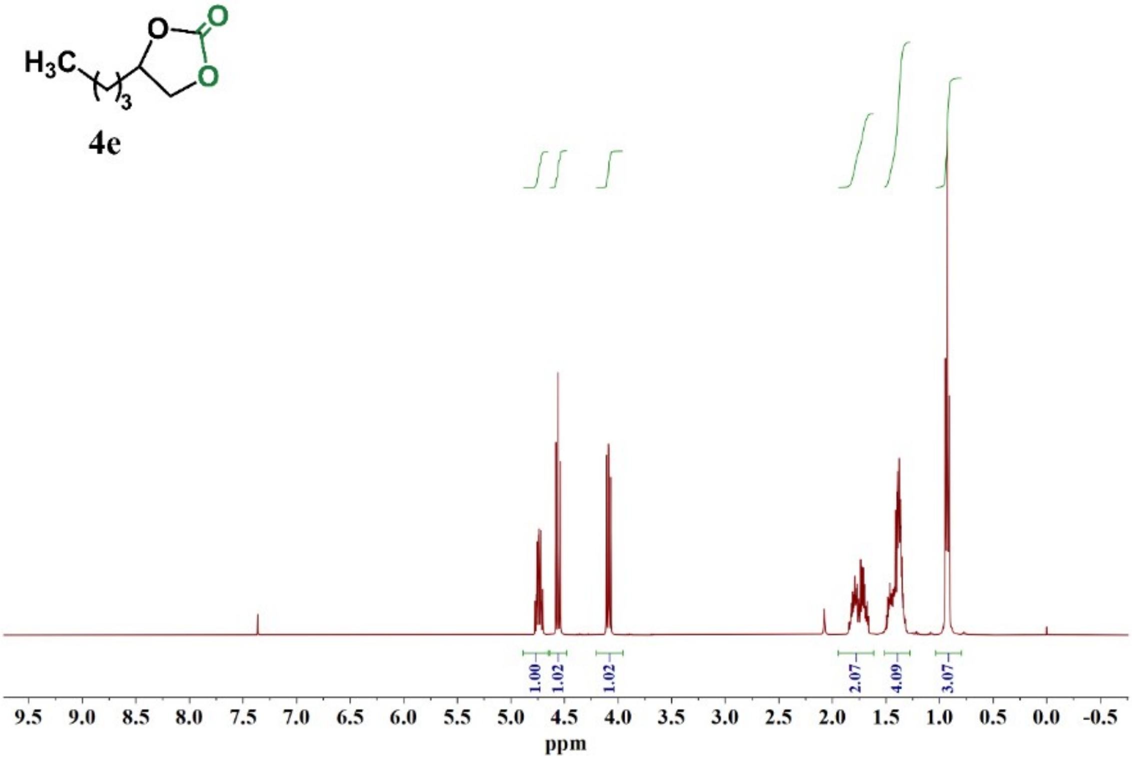

Fig. S12. [1]H NMR spectrum of **4e** (400 MHz, $CDCl_3$, 298 K).

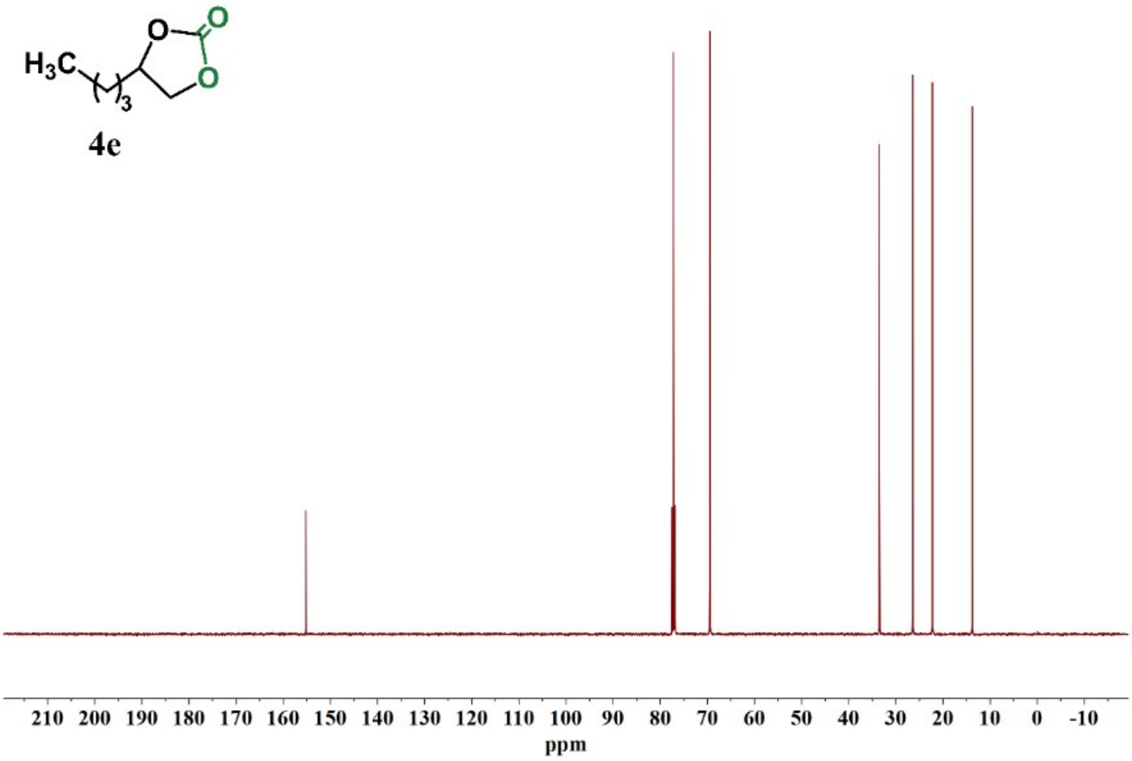

Fig. S13. [13]C NMR spectrum of **4e** (126 MHz, $CDCl_3$, 298 K).

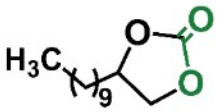

4f

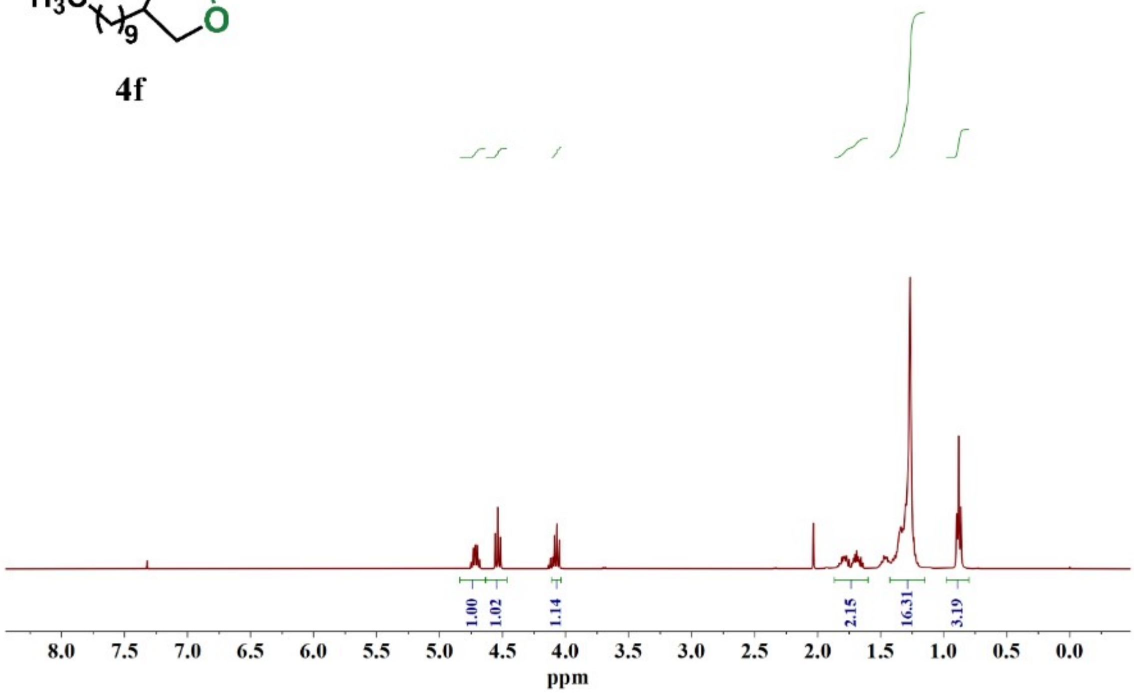

Fig. S14. ^{1}H NMR spectrum of **4f** (400 MHz, $CDCl_3$, 298 K).

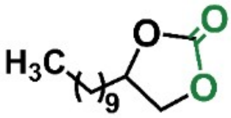

4f

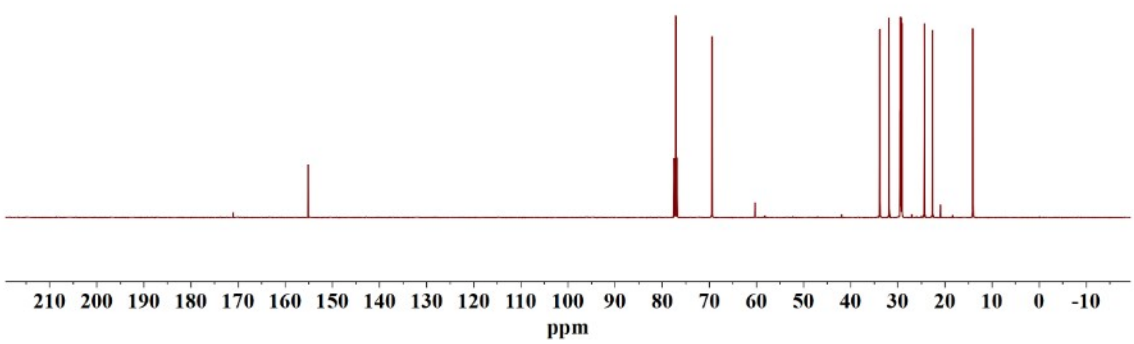

Fig. S15. ^{13}C NMR spectrum of **4f** (126 MHz, $CDCl_3$, 298 K).

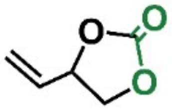

4g

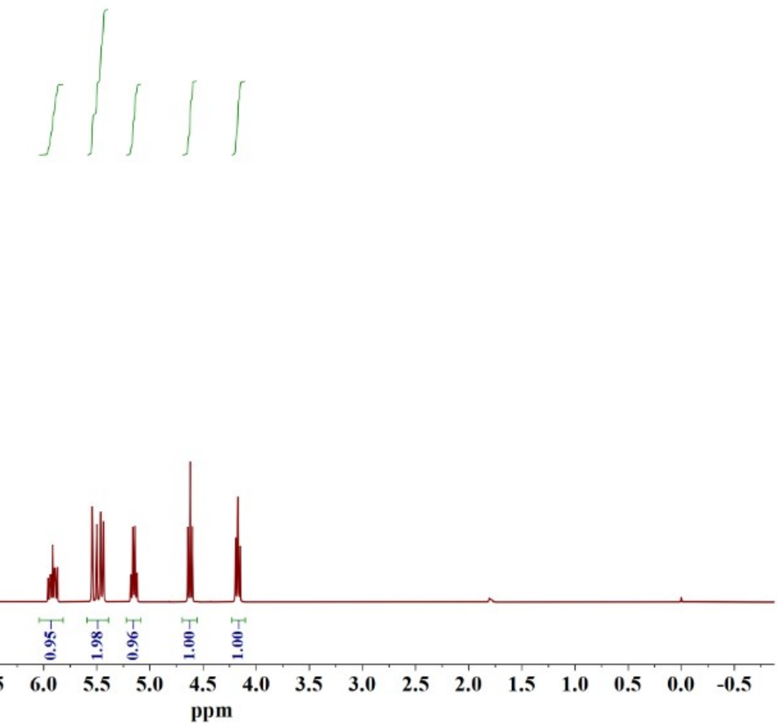

Fig. S16. ^{1}H NMR spectrum of **4g** (400 MHz, $CDCl_3$, 298 K).

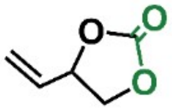

4g

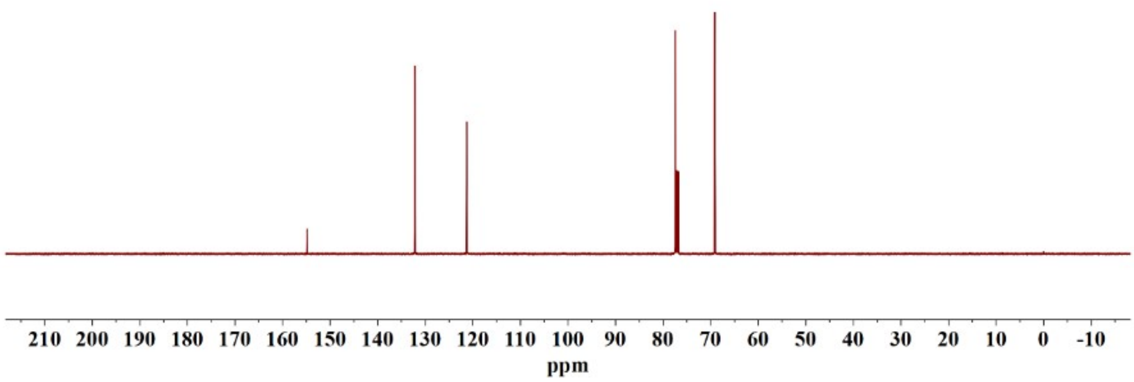

Fig. S17. ^{13}C NMR spectrum of **4g** (126 MHz, $CDCl_3$, 298 K).

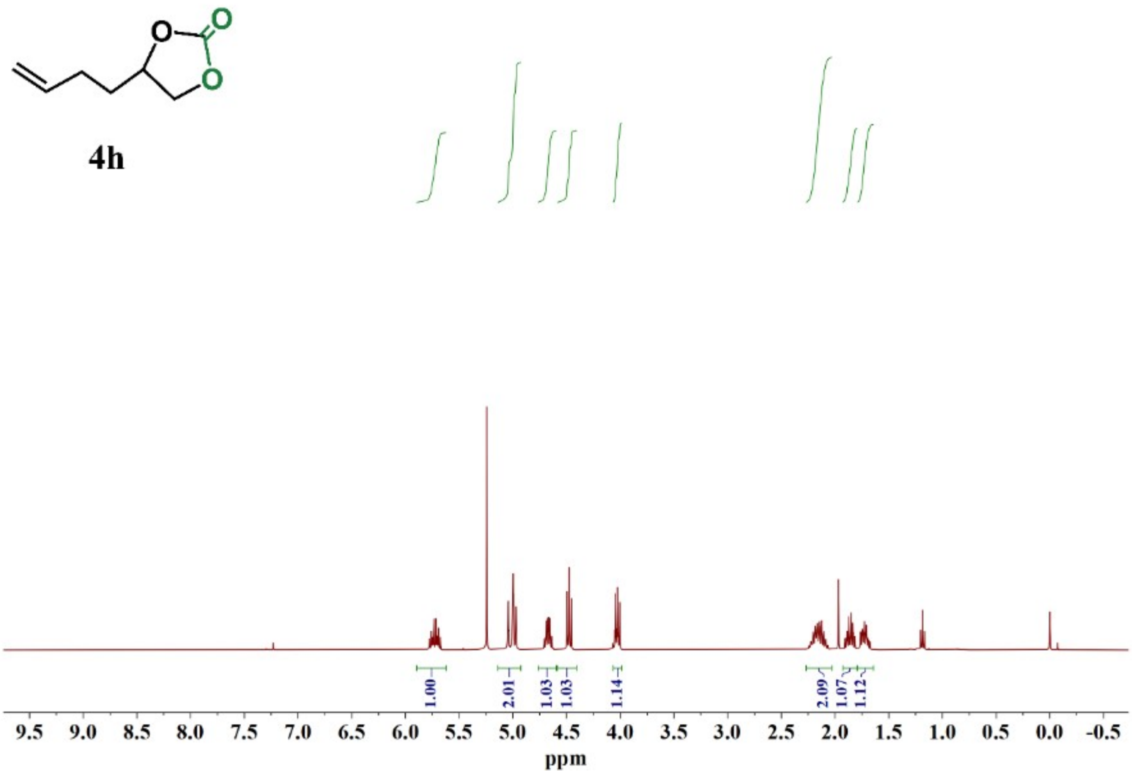

Fig. S18. ^{1}H NMR spectrum of **4h** (400 MHz, $CDCl_3$, 298 K).

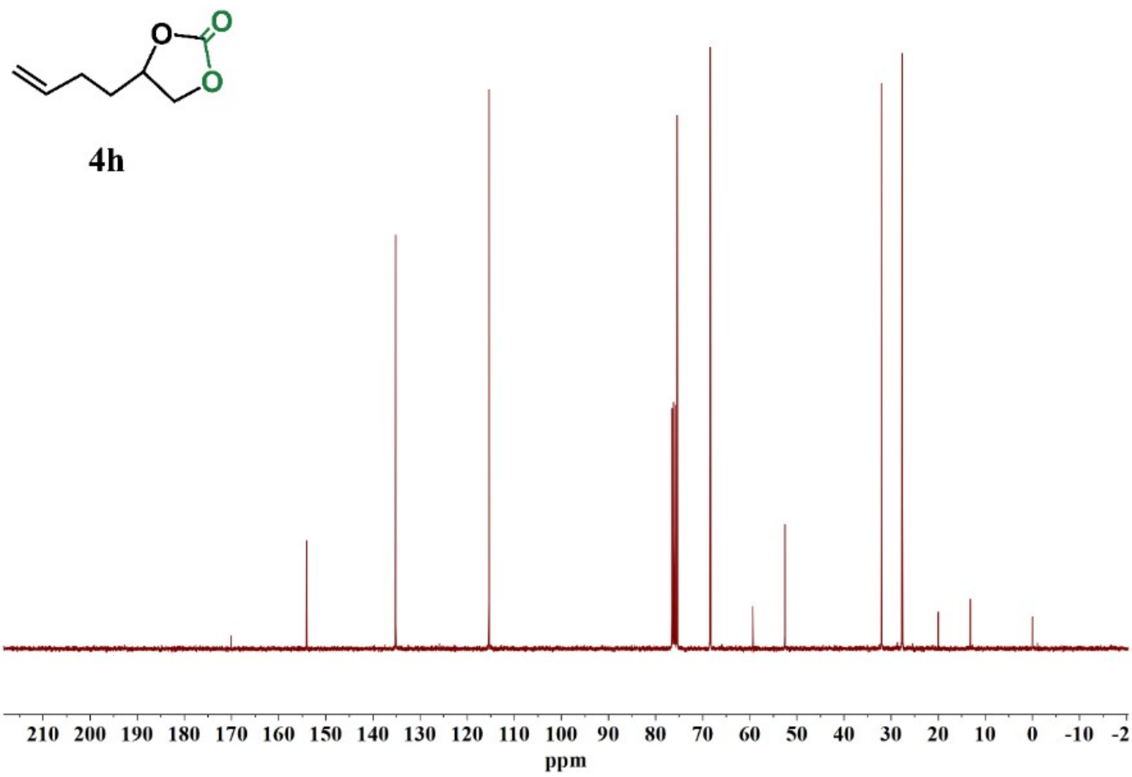

Fig. S19. ^{13}C NMR spectrum of **4h** (126 MHz, $CDCl_3$, 298 K).

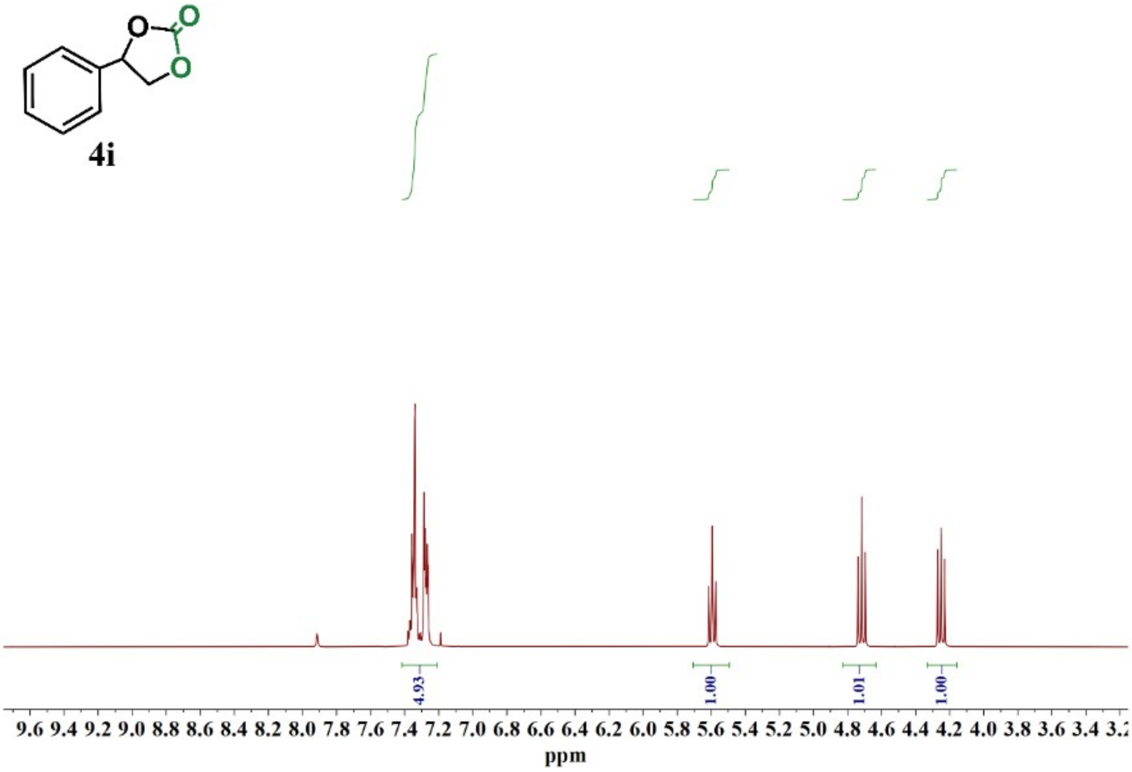

Fig. S20. ^{1}H NMR spectrum of **4i** (400 MHz, $CDCl_3$, 298 K).

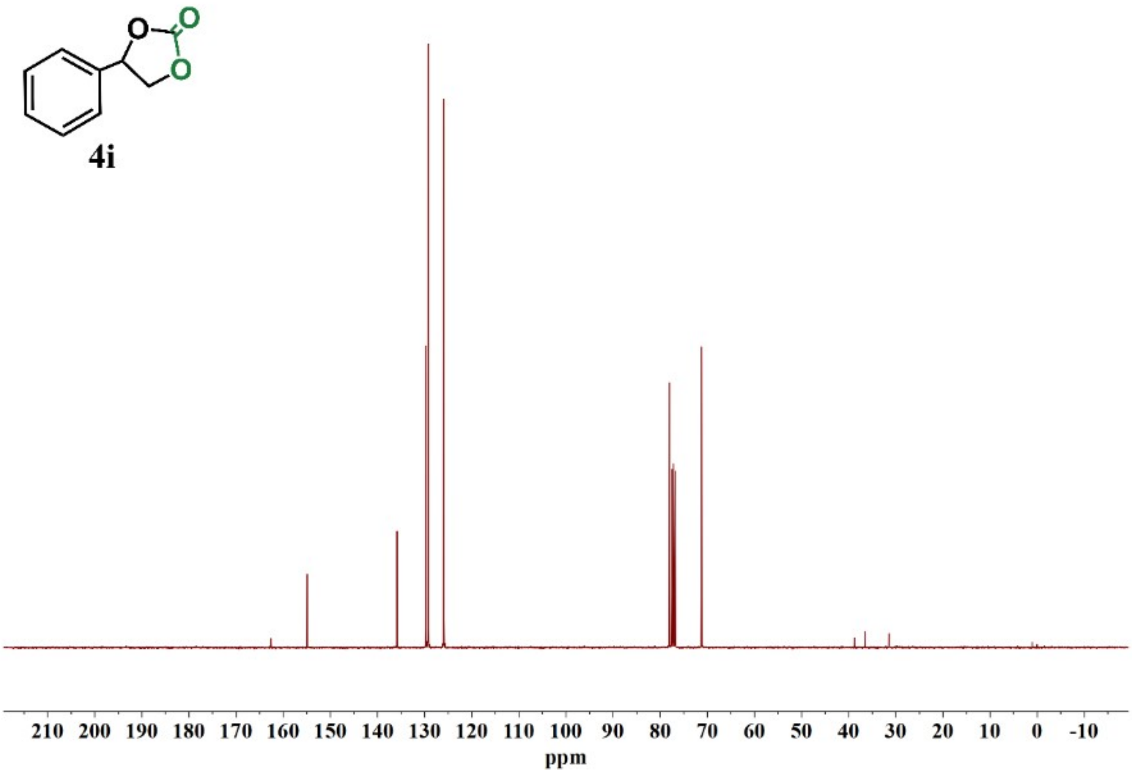

Fig. S21. ^{13}C NMR spectrum of **4i** (126 MHz, $CDCl_3$, 298 K).

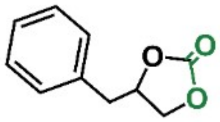

4j

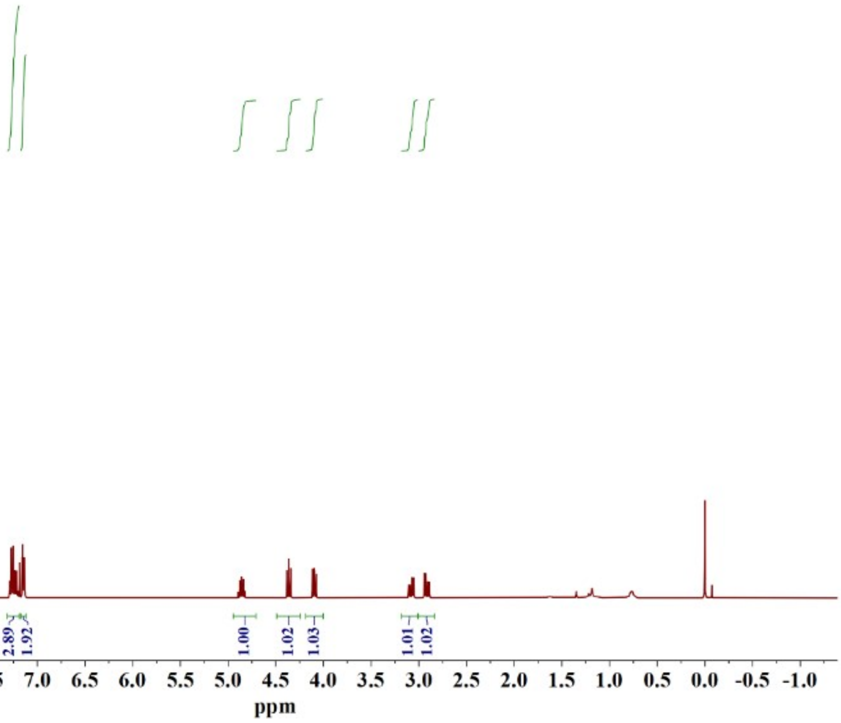

Fig. S22. ^{1}H NMR spectrum of **4j** (400 MHz, $CDCl_3$, 298 K).

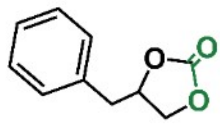

4j

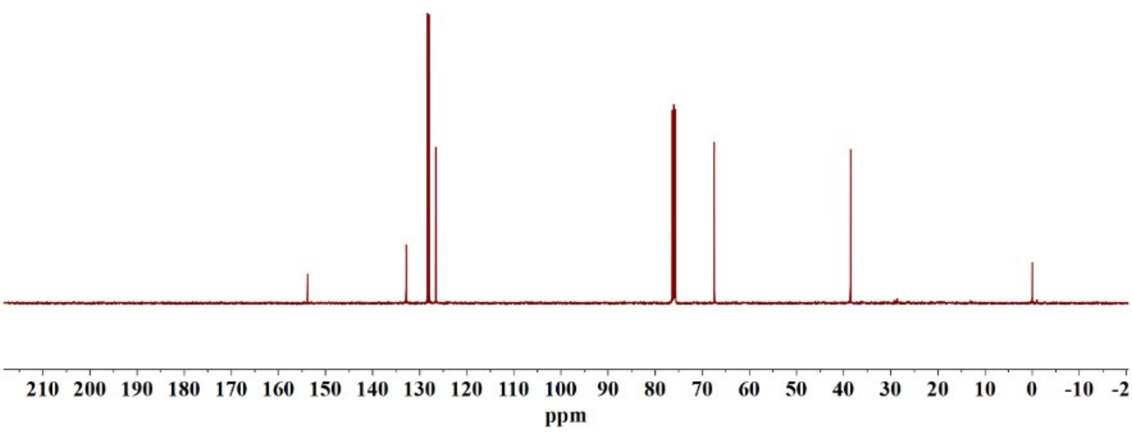

Fig. S23. ^{13}C NMR spectrum of **4j** (126 MHz, $CDCl_3$, 298 K).

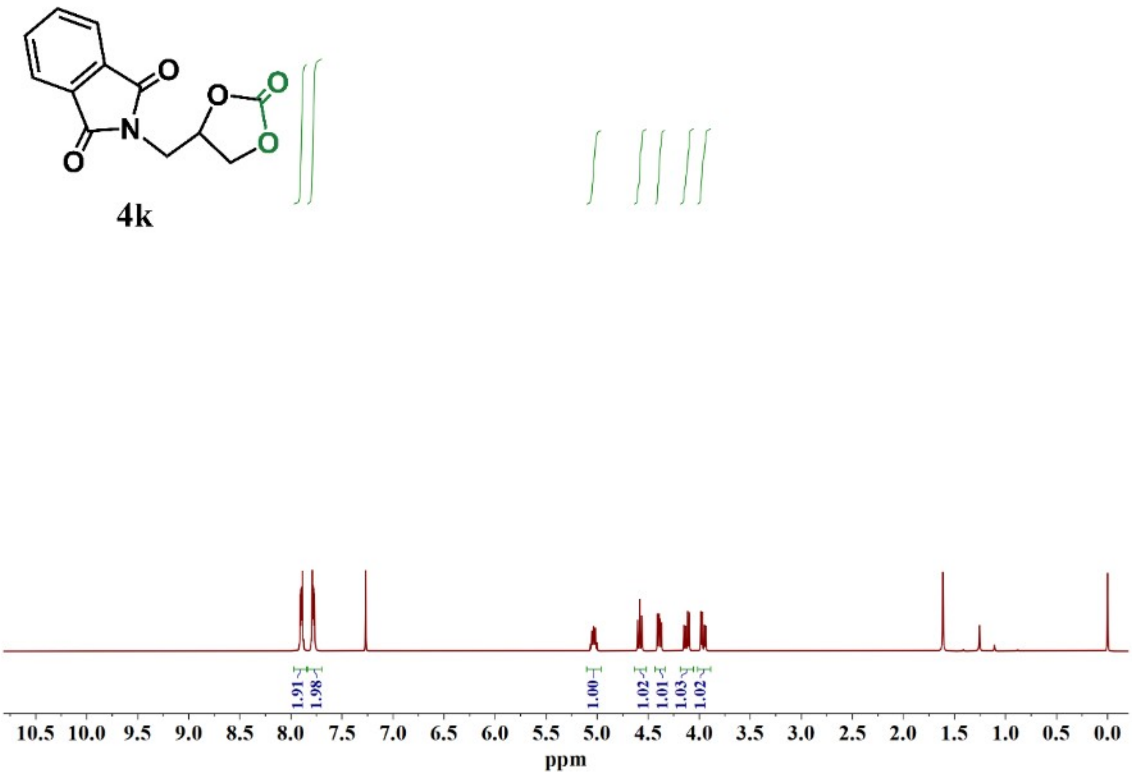

Fig. S24. ^{1}H NMR spectrum of **4k** (400 MHz, $CDCl_3$, 298 K).

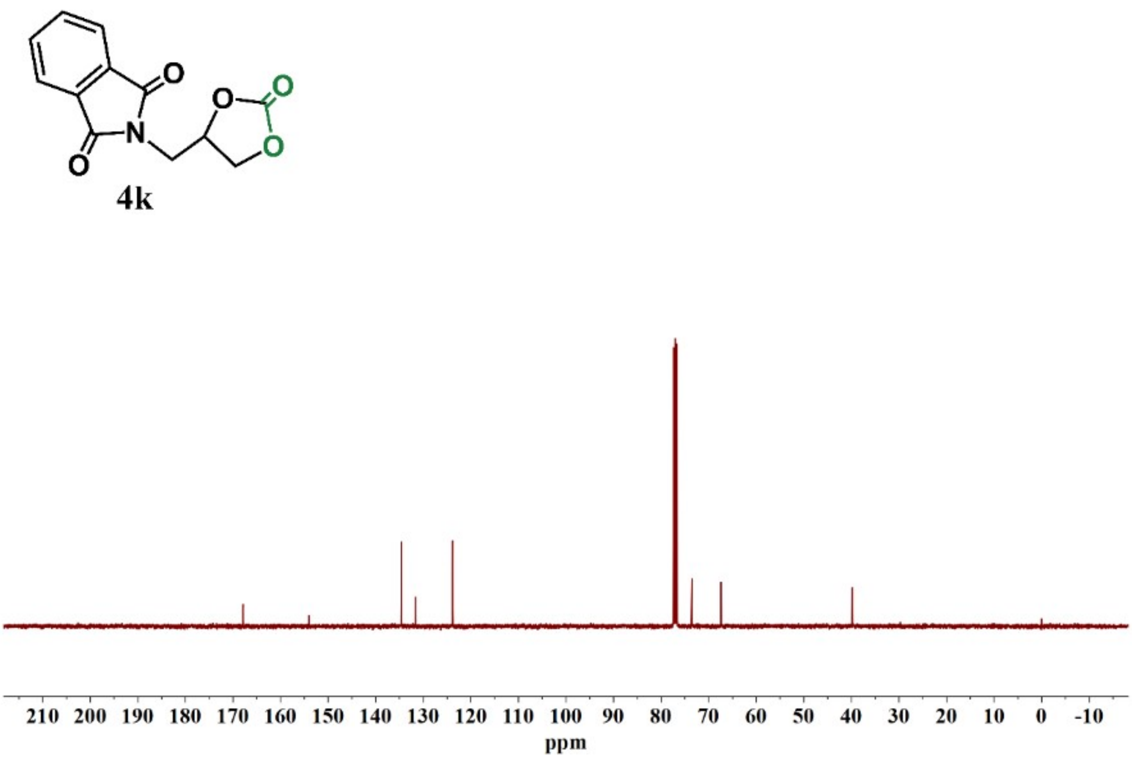

Fig. S25. ^{13}C NMR spectrum of **4k** (126 MHz, $CDCl_3$, 298 K).

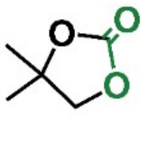

4l

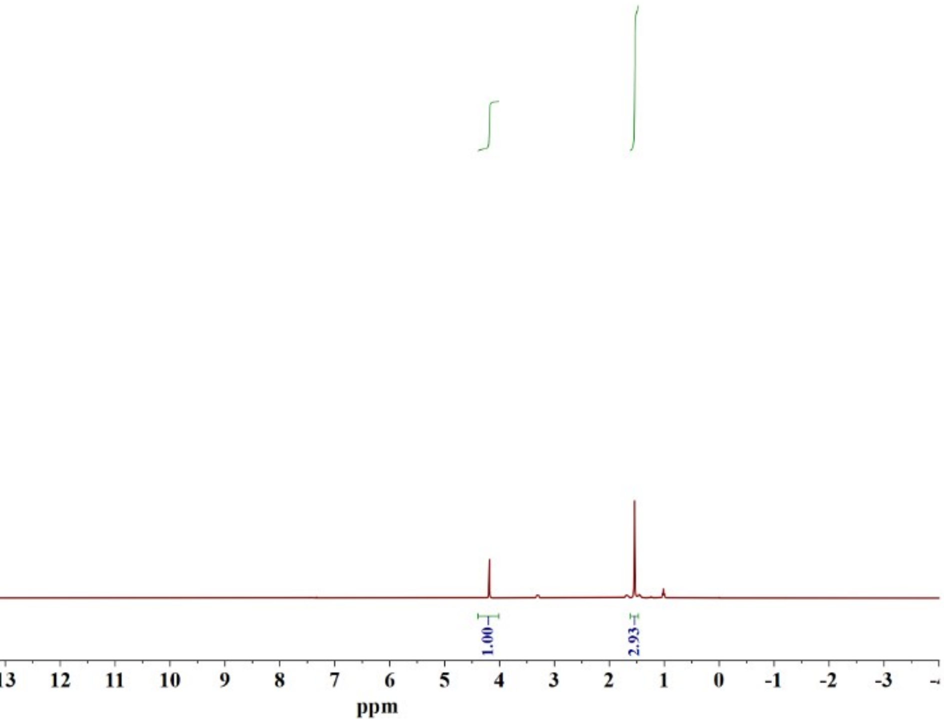

Fig. S26. ^{1}H NMR spectrum of **4l** (400 MHz, $CDCl_3$, 298 K).

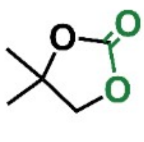

4l

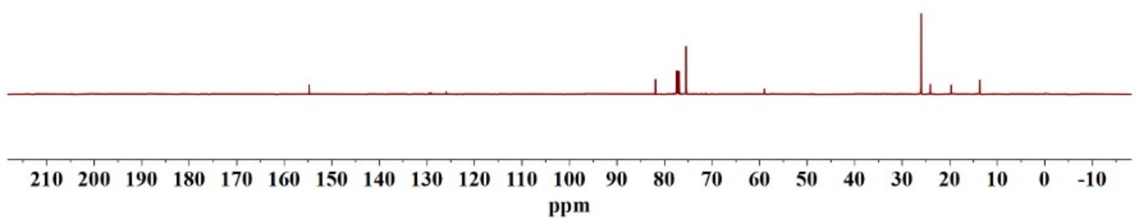

Fig. S27. ^{13}C NMR spectrum of **4l** (126 MHz, $CDCl_3$, 298 K).

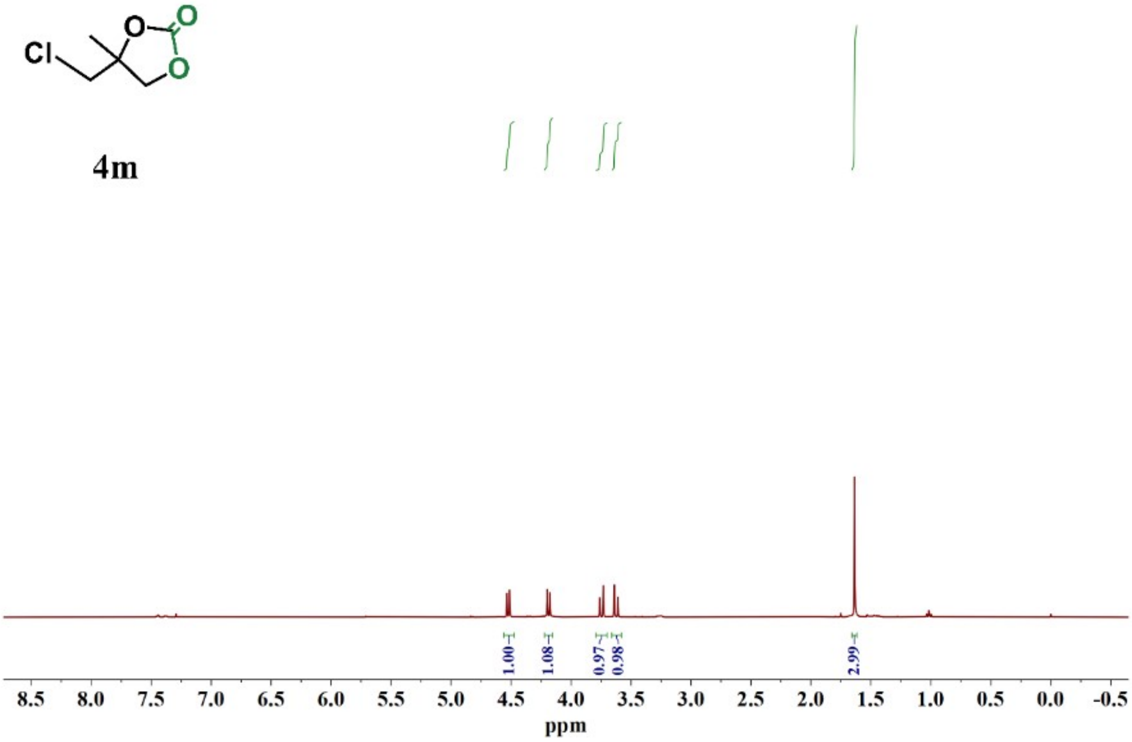

Fig. S28. ^{1}H NMR spectrum of **4m** (400 MHz, $CDCl_3$, 298 K).

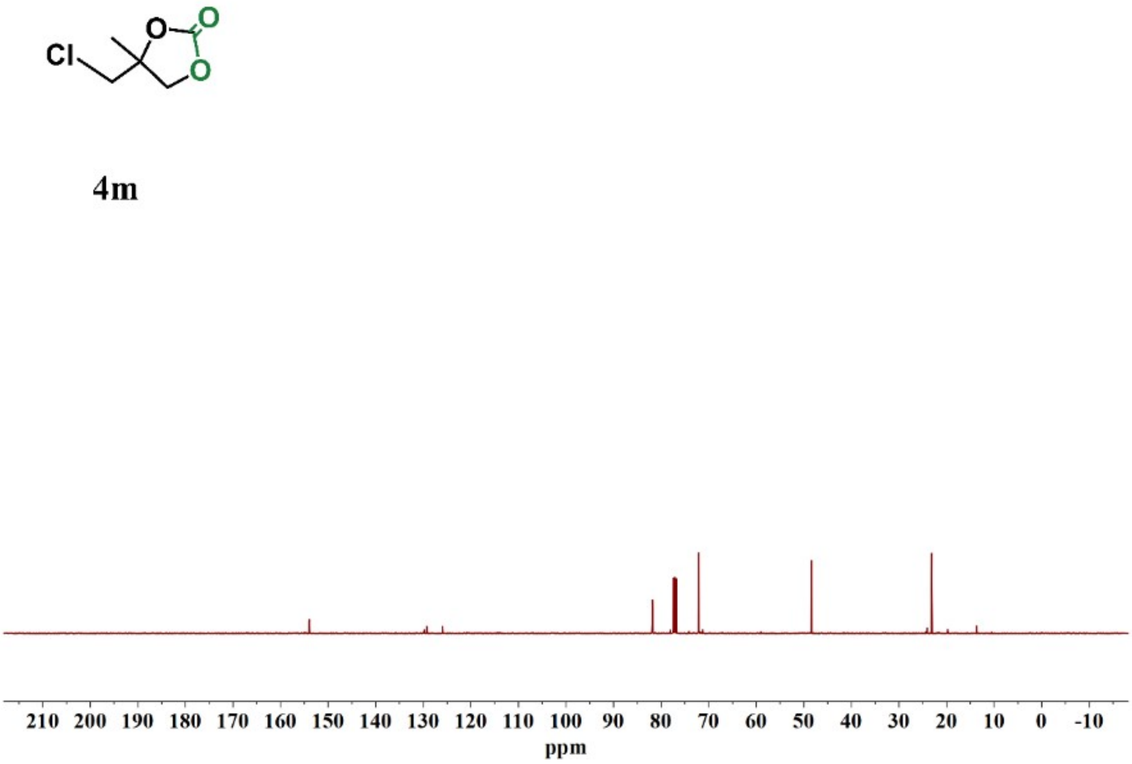

Fig. S29. ^{13}C NMR spectrum of **4m** (126 MHz, $CDCl_3$, 298 K).

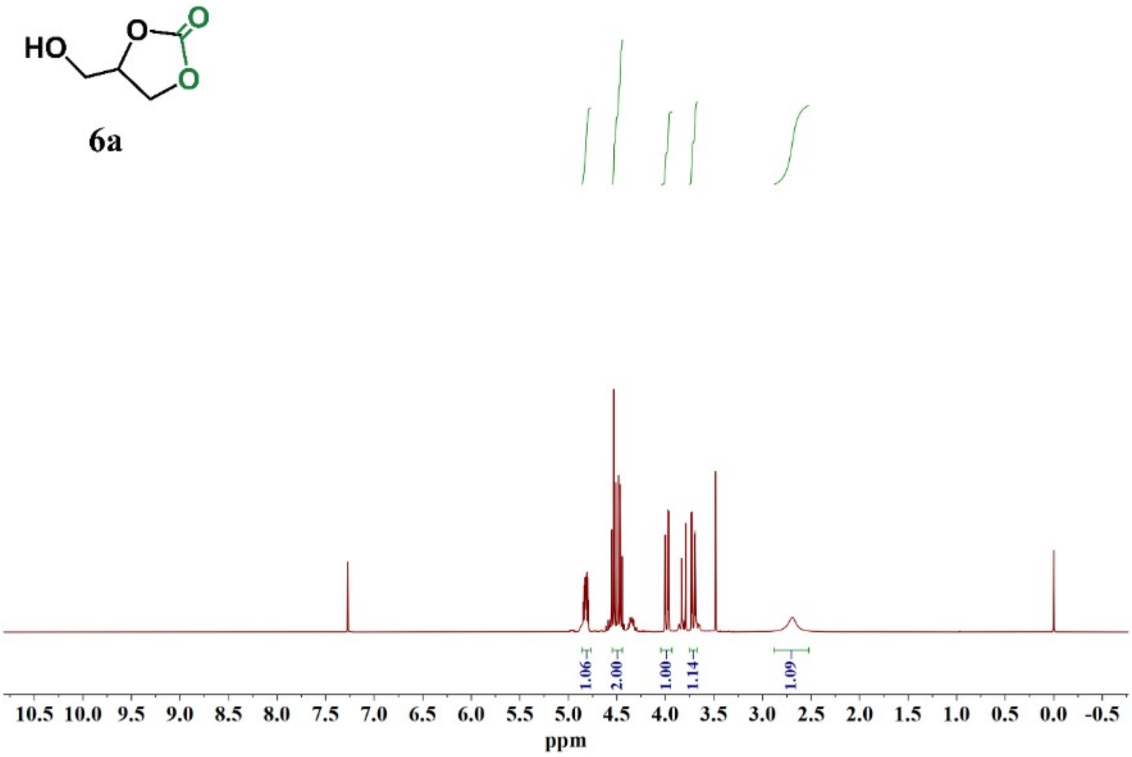

Fig. S30. ^{1}H NMR spectrum of **6a** (400 MHz, $CDCl_3$, 298 K).

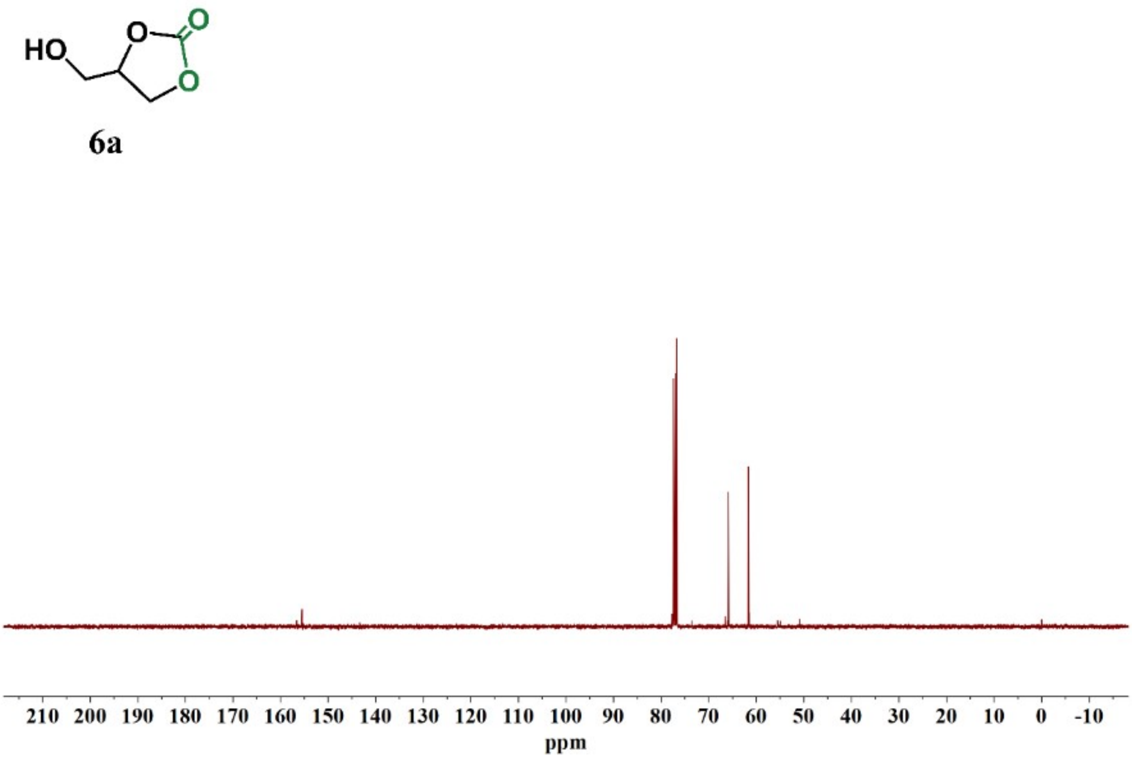

Fig. S31. ^{13}C NMR spectrum of **6a** (126 MHz, $CDCl_3$, 298 K).

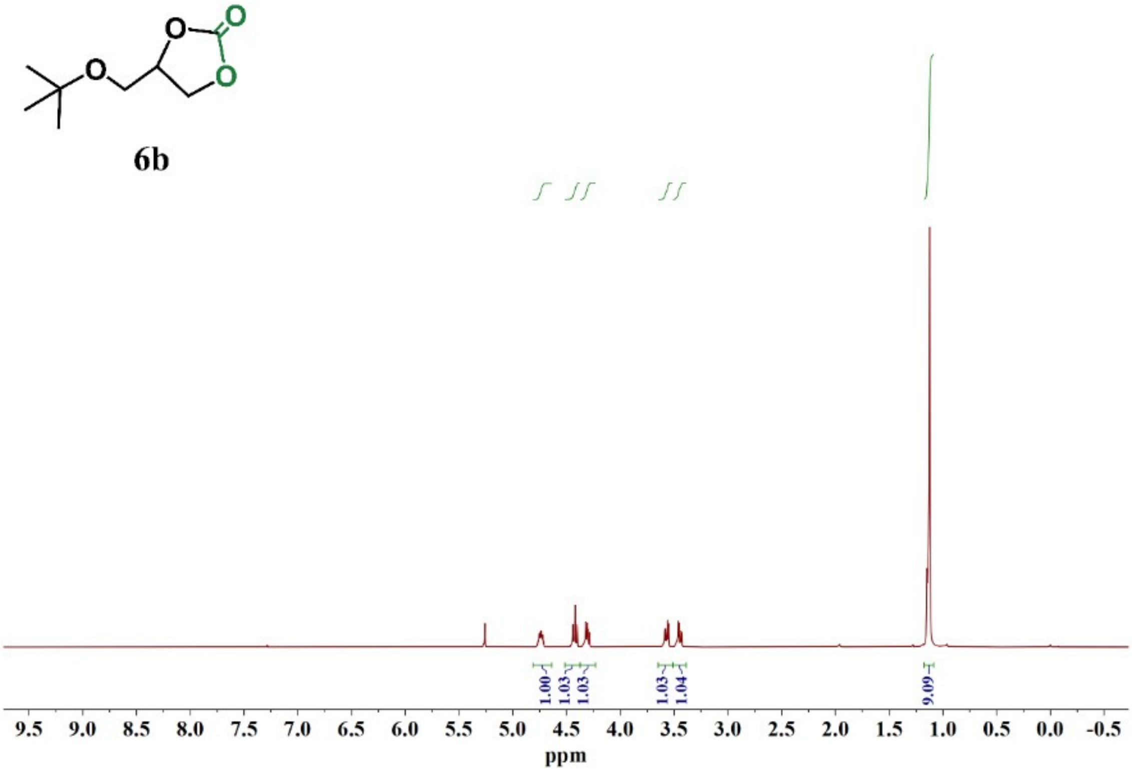

Fig. S32. ^{1}H NMR spectrum of **6b** (400 MHz, $CDCl_3$, 298 K).

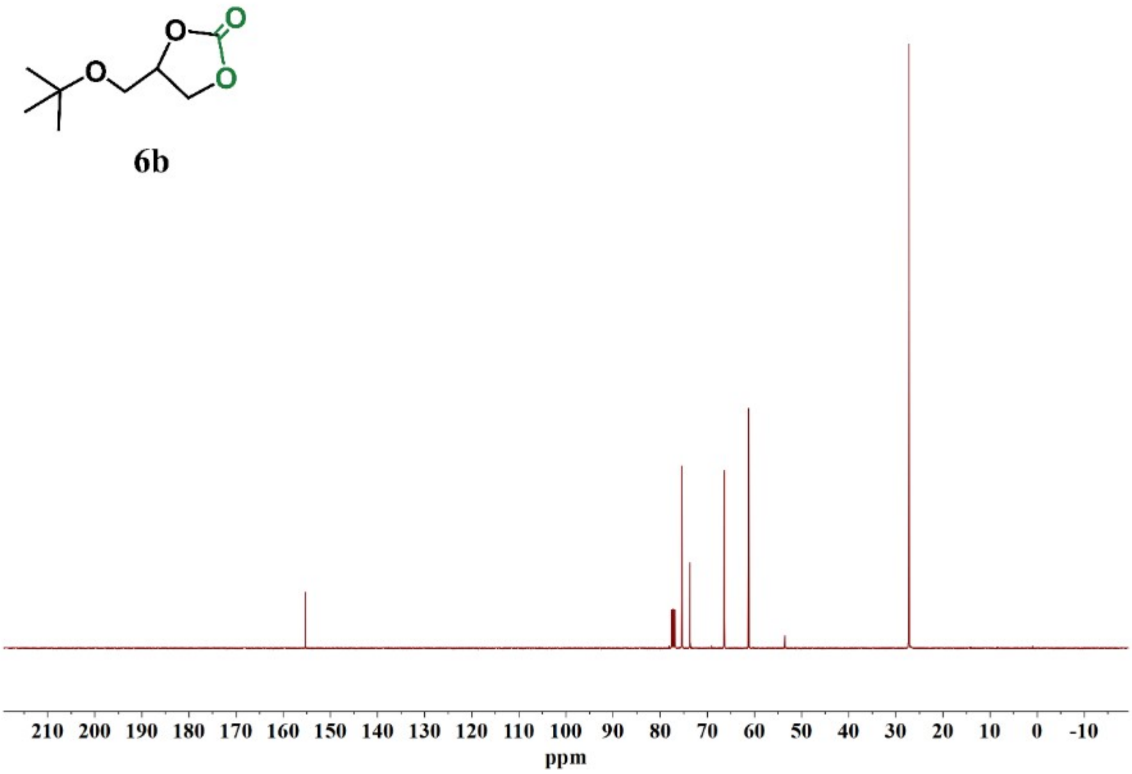

Fig. S33. ^{13}C NMR spectrum of **6b** (126 MHz, $CDCl_3$, 298 K).

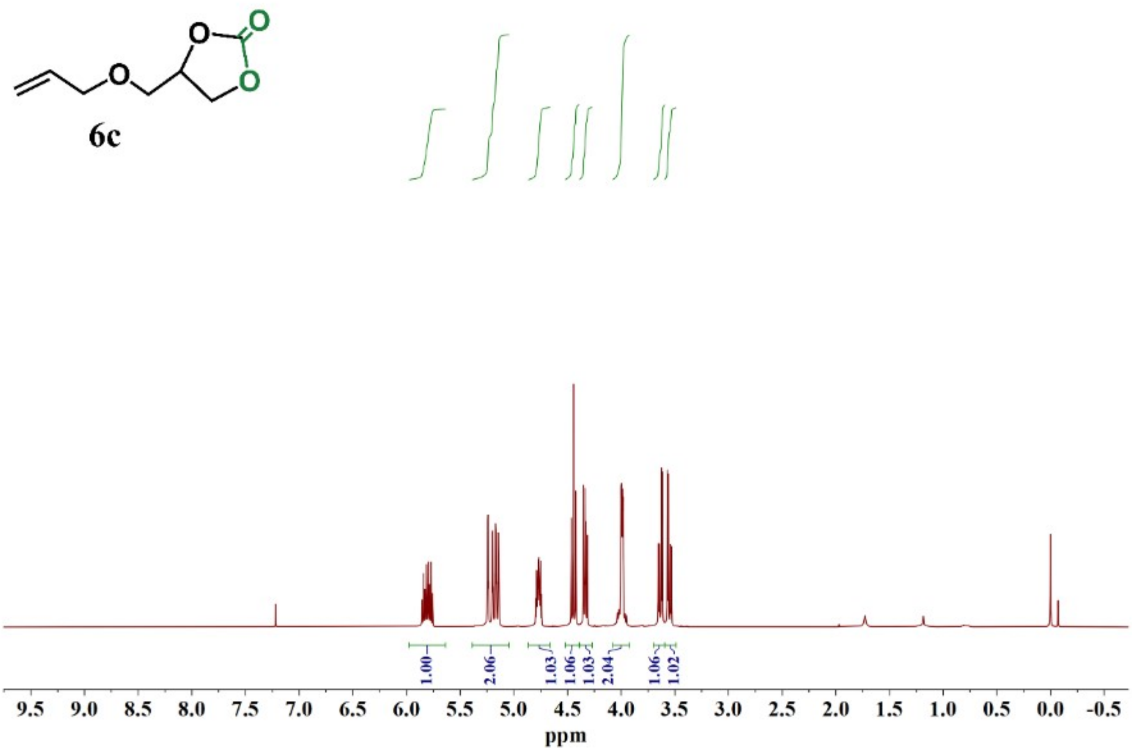

Fig. S34. ^{1}H NMR spectrum of **6c** (400 MHz, $CDCl_3$, 298 K).

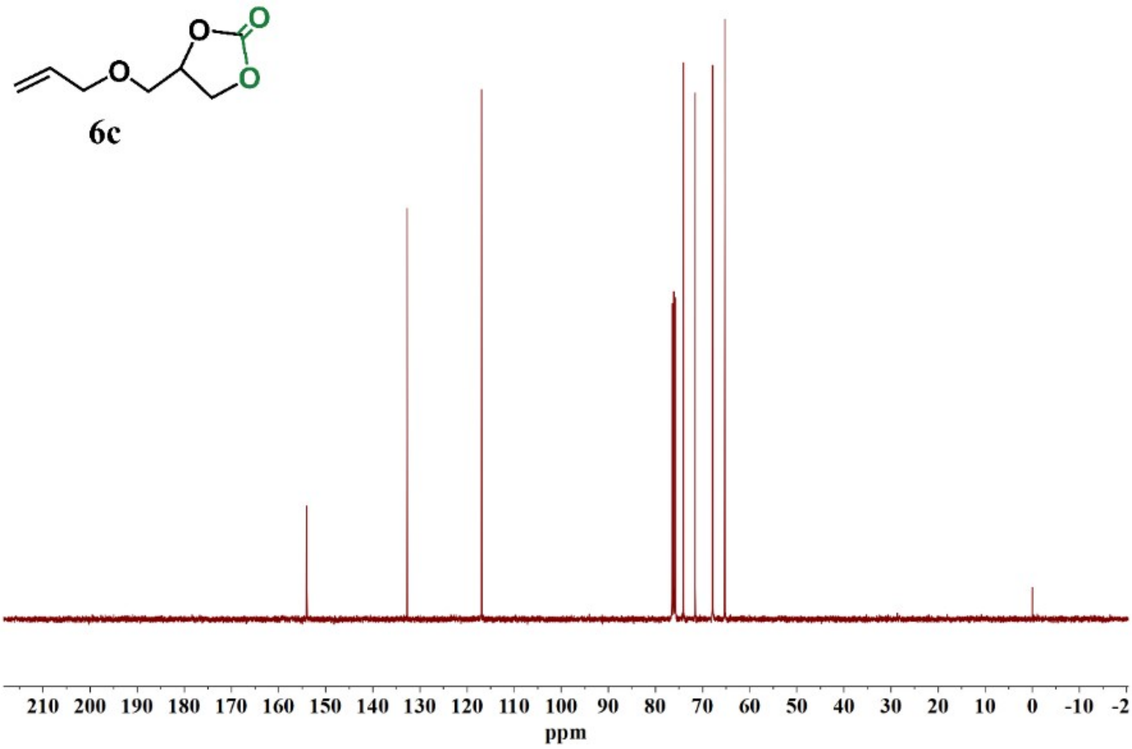

Fig. S35. ^{13}C NMR spectrum of **6c** (126 MHz, $CDCl_3$, 298 K).

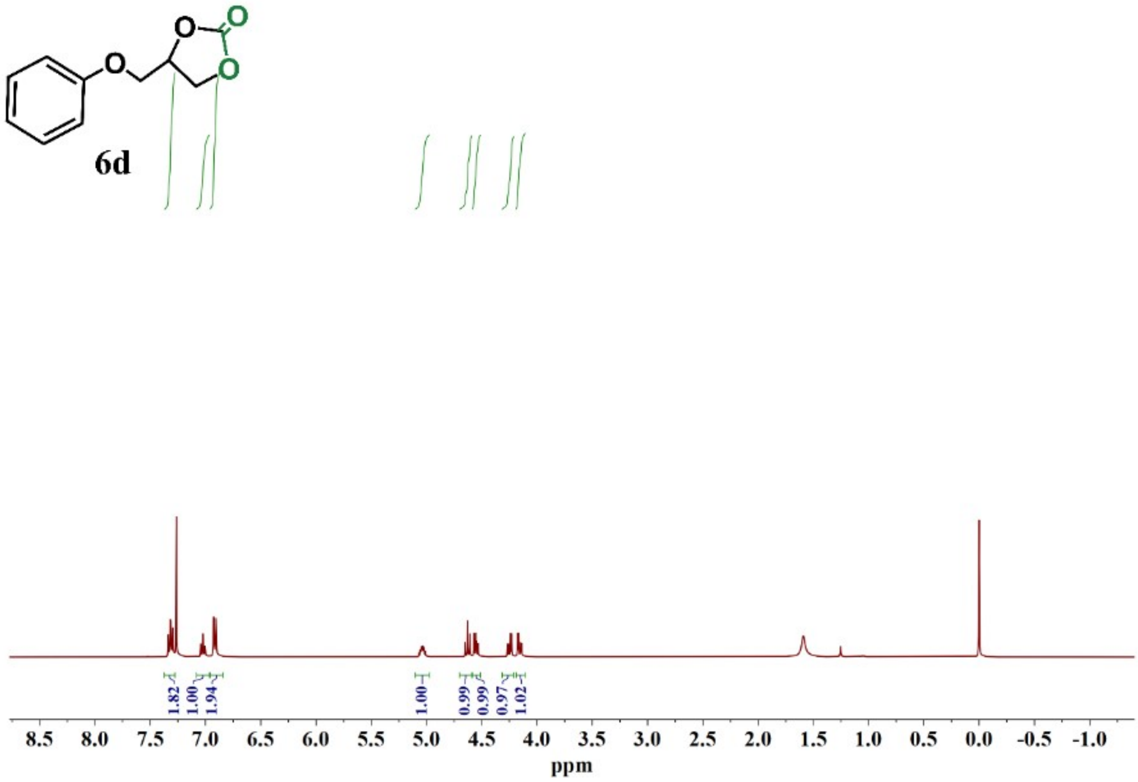

Fig. S36. ^{1}H NMR spectrum of **6d** (400 MHz, DMSO, 298 K).

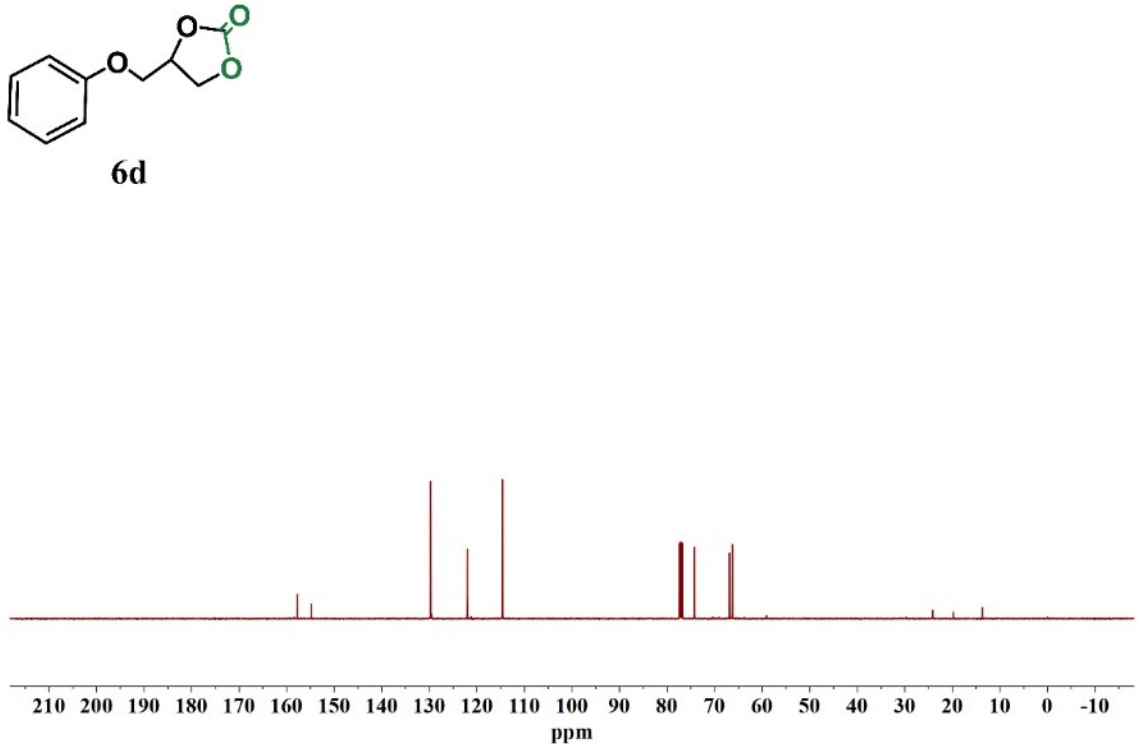

Fig. S37. ^{13}C NMR spectrum of **6d** (126 MHz, DMSO, 298 K).

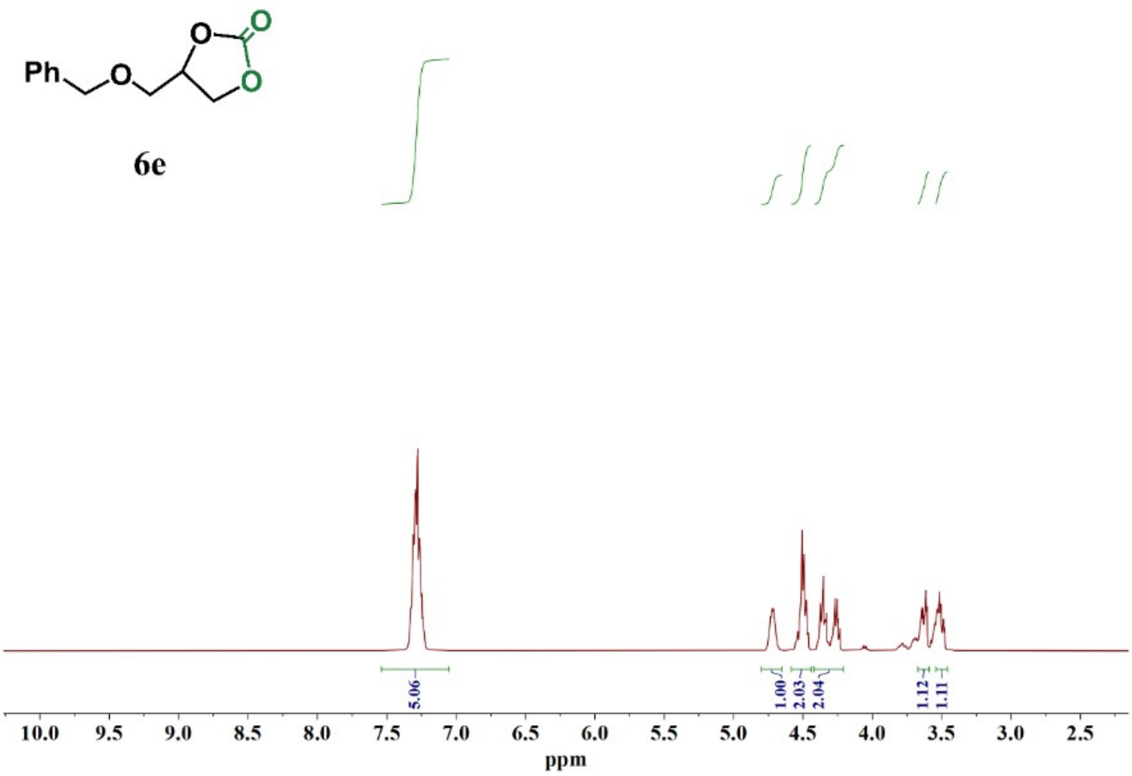

Fig. S38. ^{1}H NMR spectrum of **6e** (400 MHz, $CDCl_3$, 298 K).

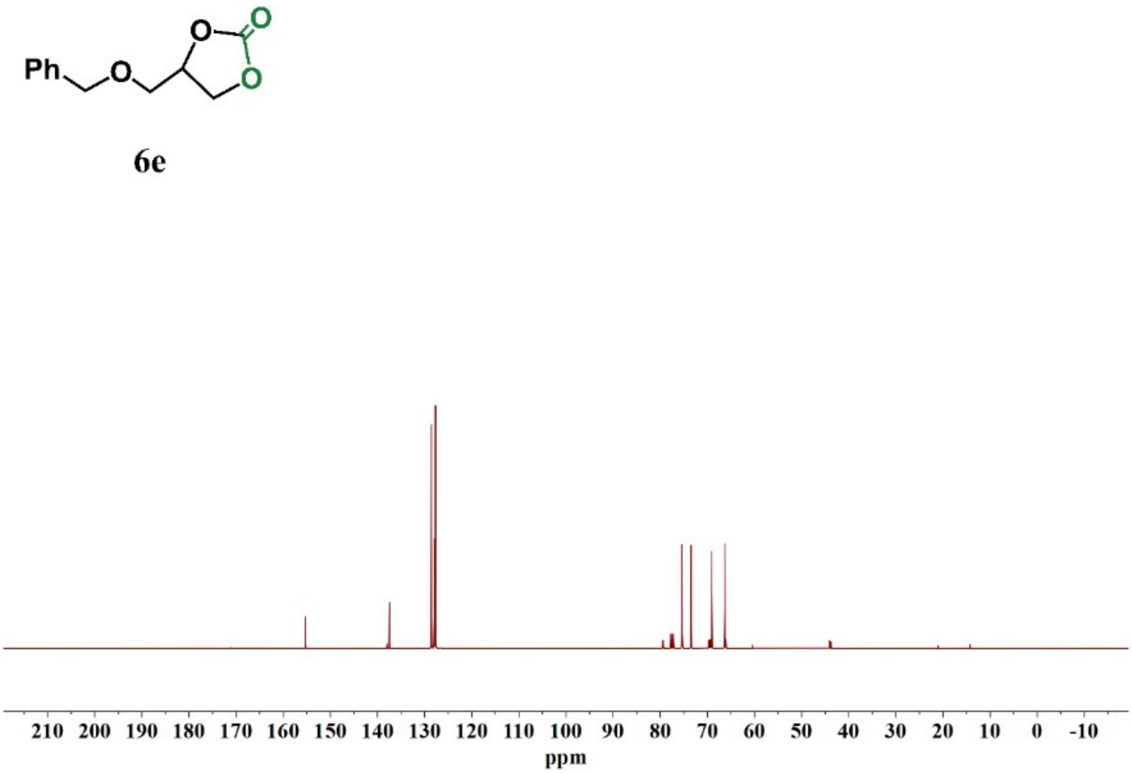

Fig. S39. ^{13}C NMR spectrum of **6e** (126 MHz, $CDCl_3$, 298 K).

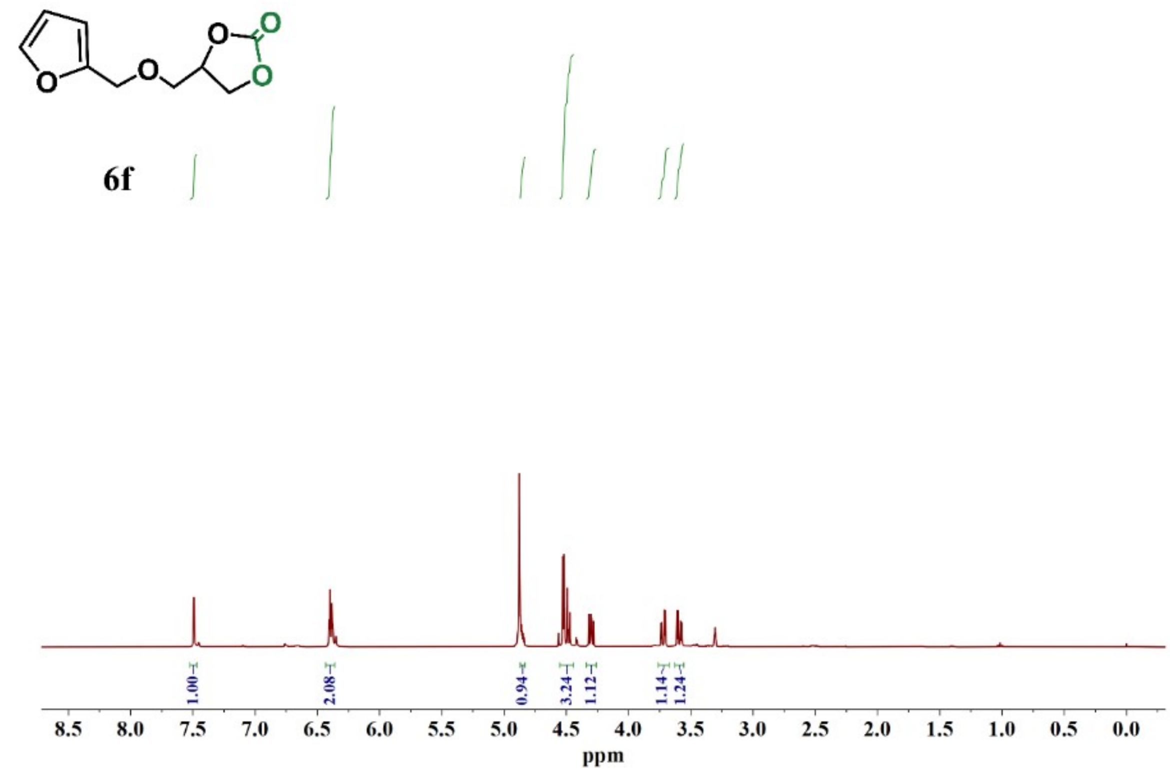

Fig. S40. ^{1}H NMR spectrum of **6f** (400 MHz, $CDCl_3$, 298 K).

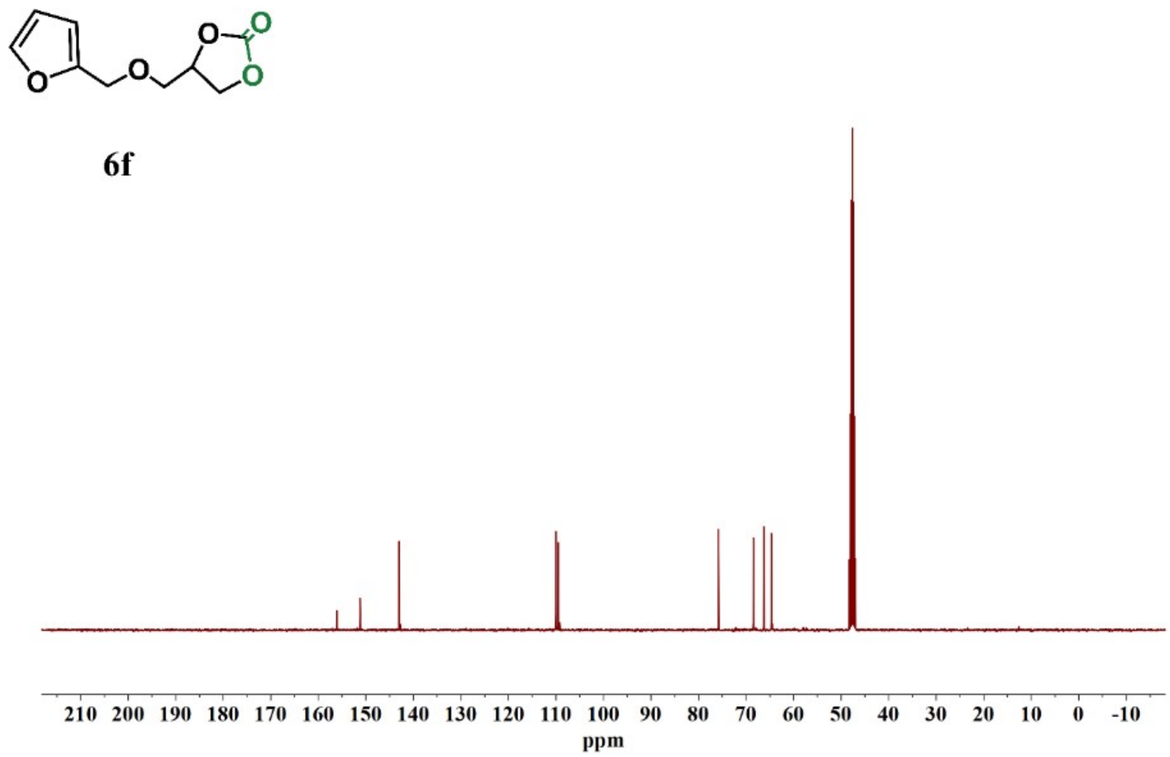

Fig. S41. ^{13}C NMR spectrum of **6f** (126 MHz, $CDCl_3$, 298 K).

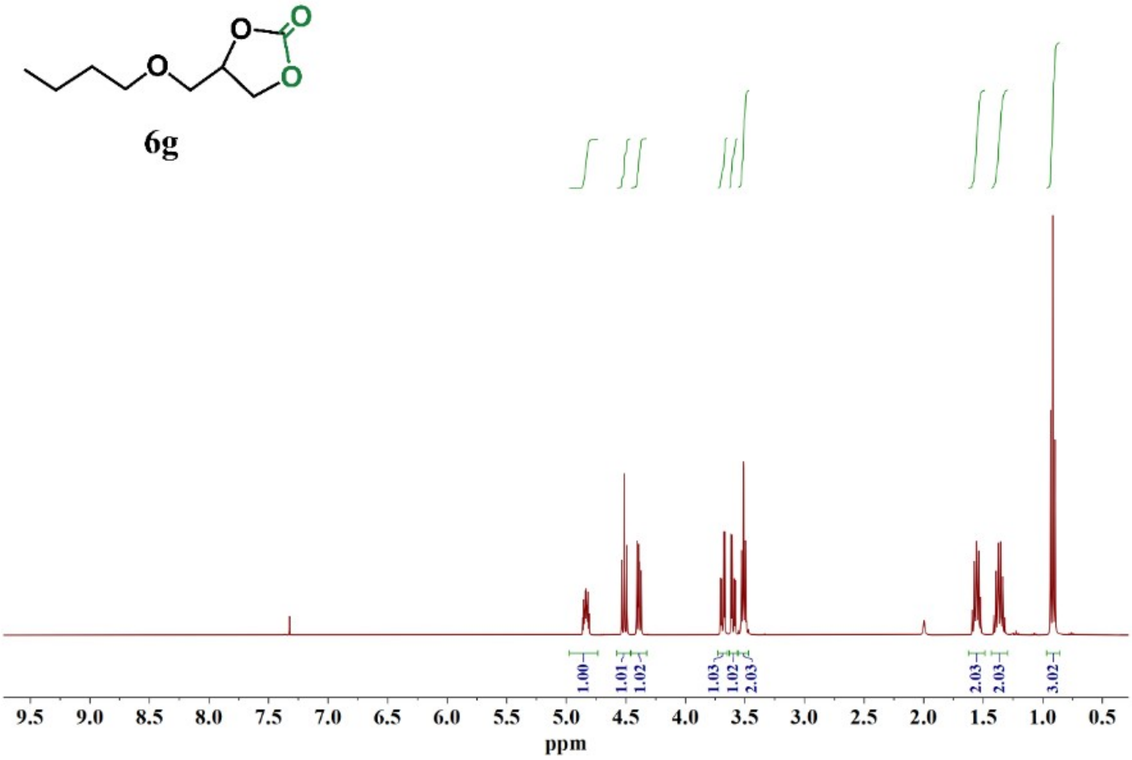

Fig. S42. ^{1}H NMR spectrum of **6g** (400 MHz, $CDCl_3$, 298 K).

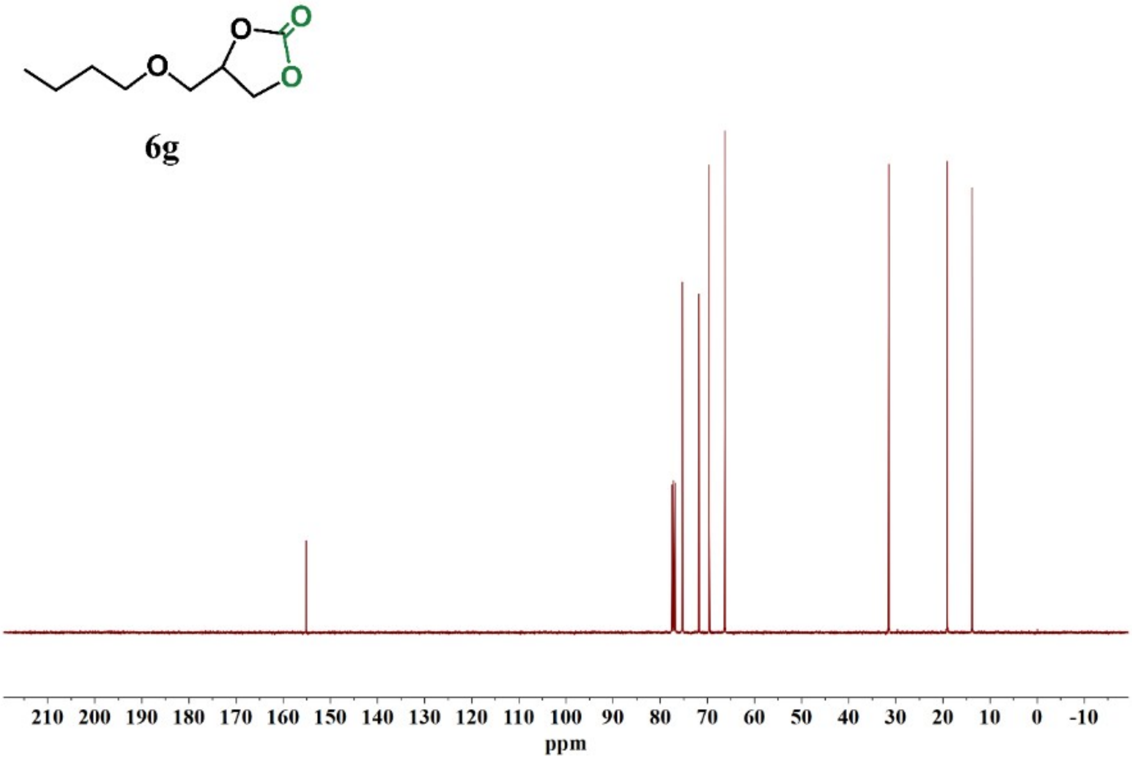

Fig. S43. ^{13}C NMR spectrum of **6g** (126 MHz, $CDCl_3$, 298 K).

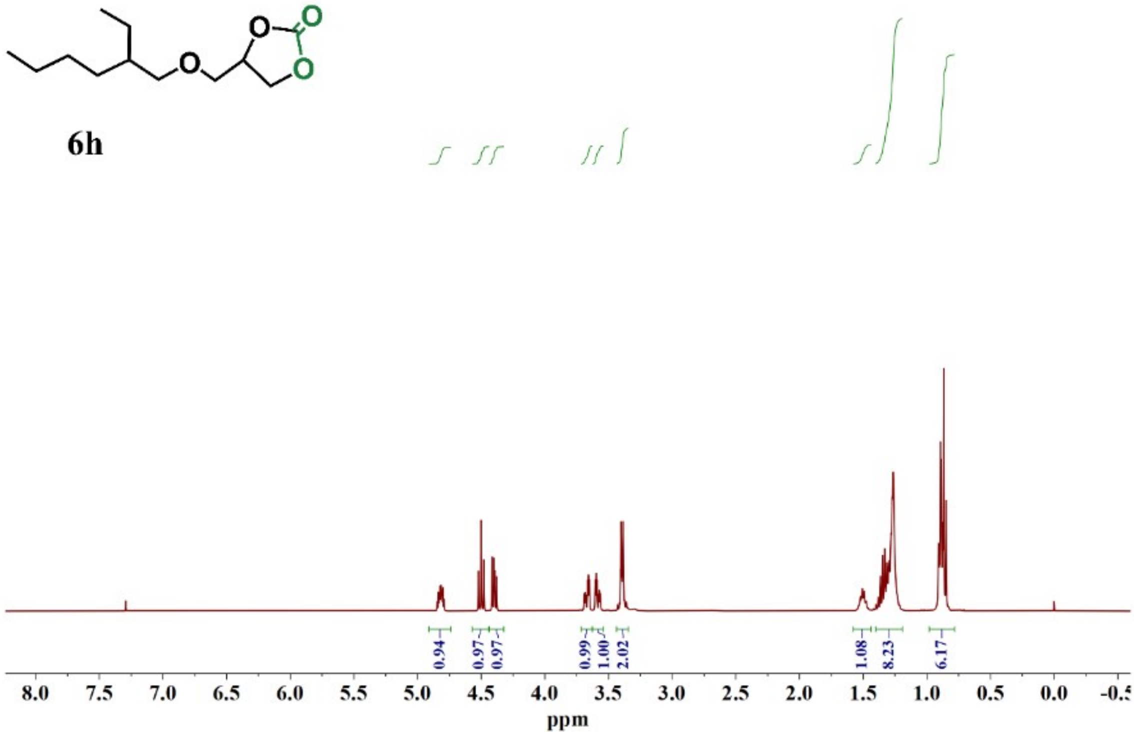

6h

Fig. S44. ^{1}H NMR spectrum of **6h** (400 MHz, $CDCl_3$, 298 K).

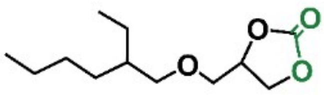

6h

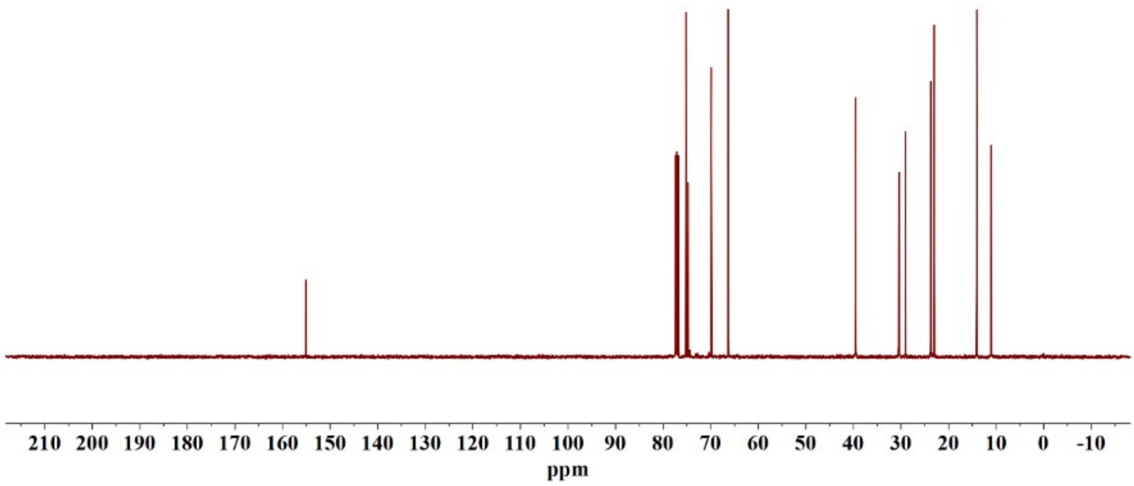

Fig. S45. ^{13}C NMR spectrum of **6h** (126 MHz, $CDCl_3$, 298 K).

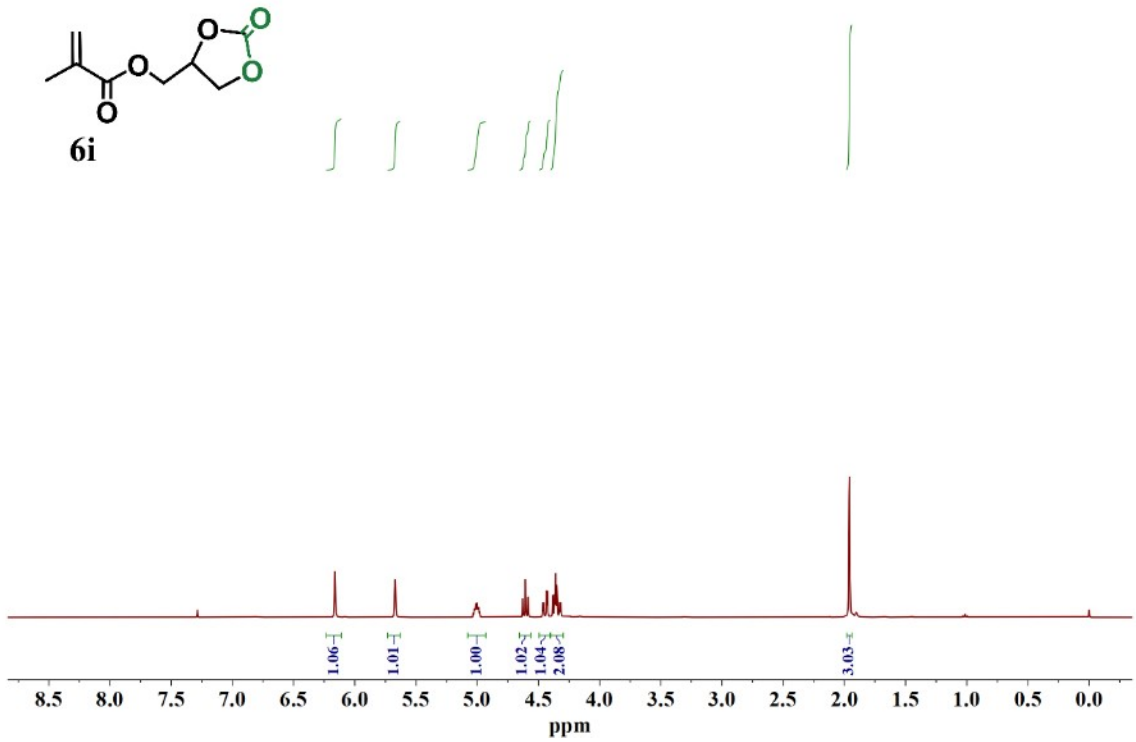

Fig. S46. ^{1}H NMR spectrum of **6i** (400 MHz, $CDCl_3$, 298 K).

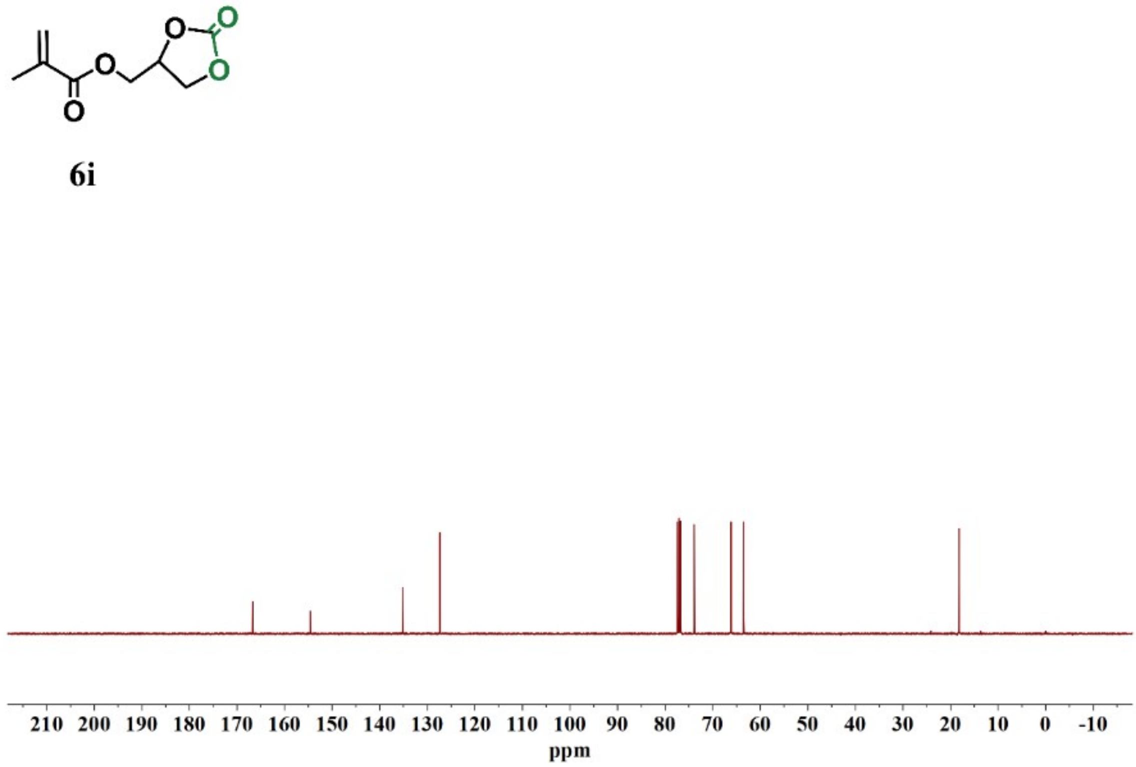

Fig. S47. ^{13}C NMR spectrum of **6i** (126 MHz, $CDCl_3$, 298 K).

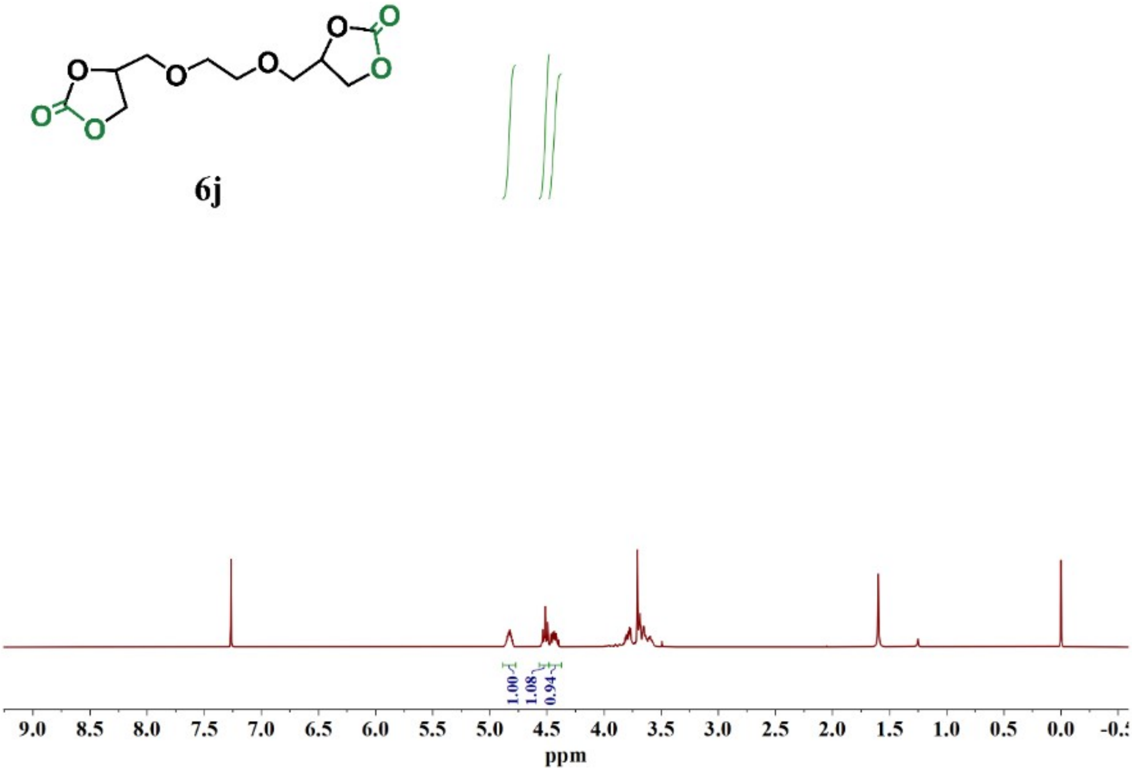

Fig. S48. ^{1}H NMR spectrum of **6j** (400 MHz, $CDCl_3$, 298 K).

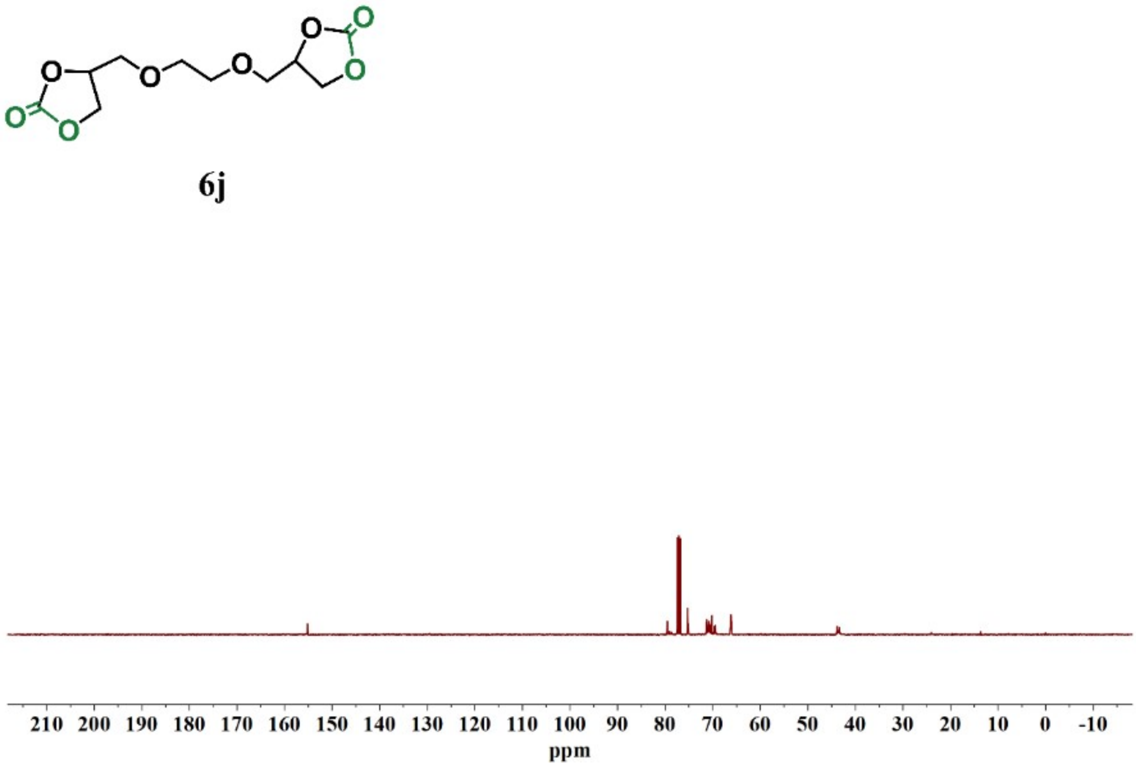

Fig. S49. ^{13}C NMR spectrum of **6j** (126 MHz, $CDCl_3$, 298 K).

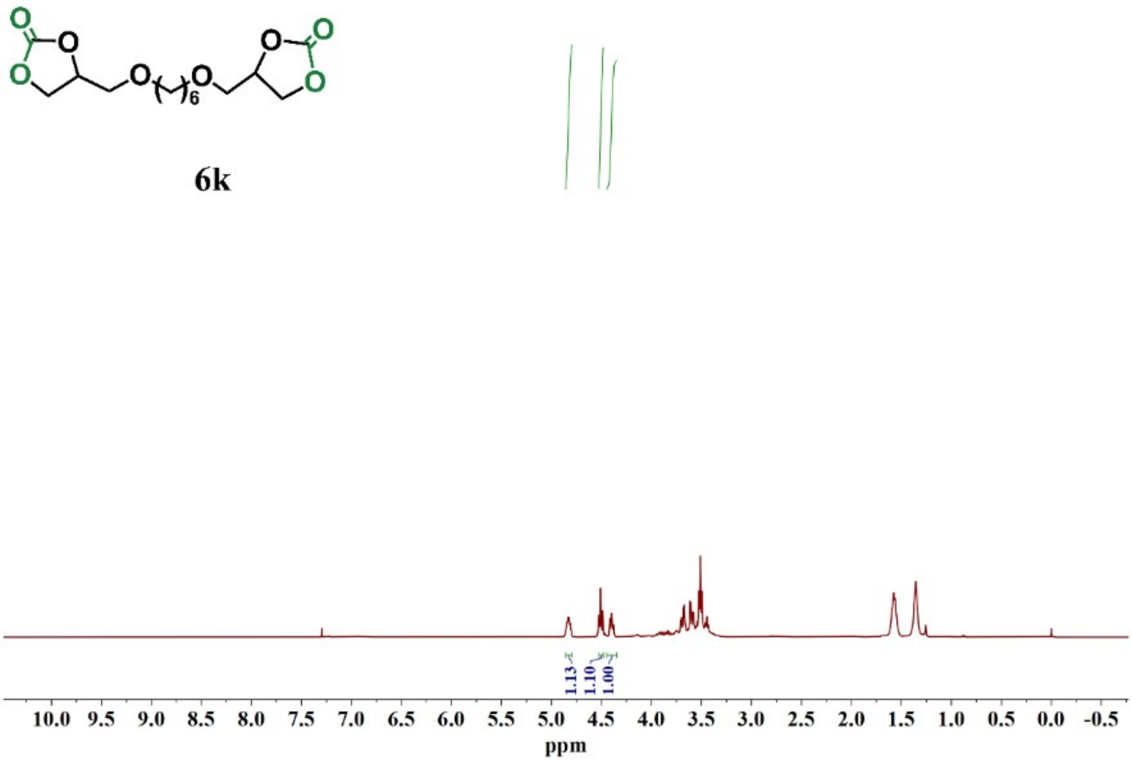

Fig. S50. ^{1}H NMR spectrum of **6k** (400 MHz, $CDCl_3$, 298 K).

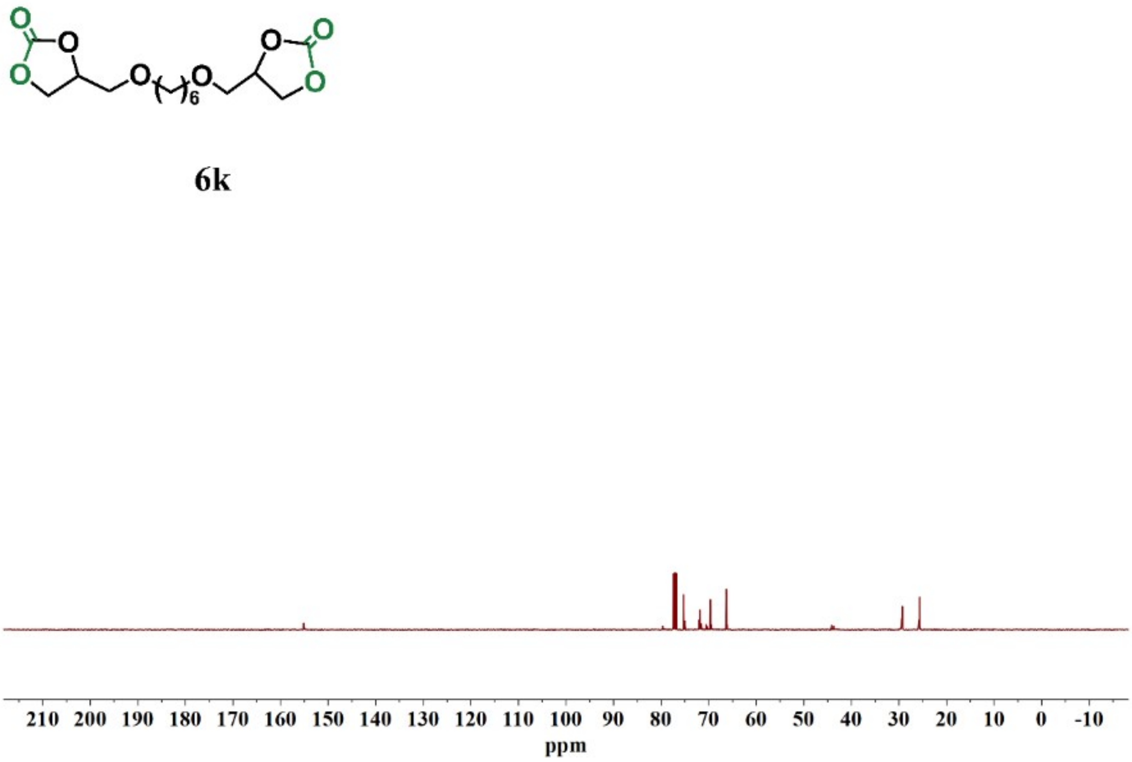

Fig. S51. ^{13}C NMR spectrum of **6k** (126 MHz, $CDCl_3$, 298 K).

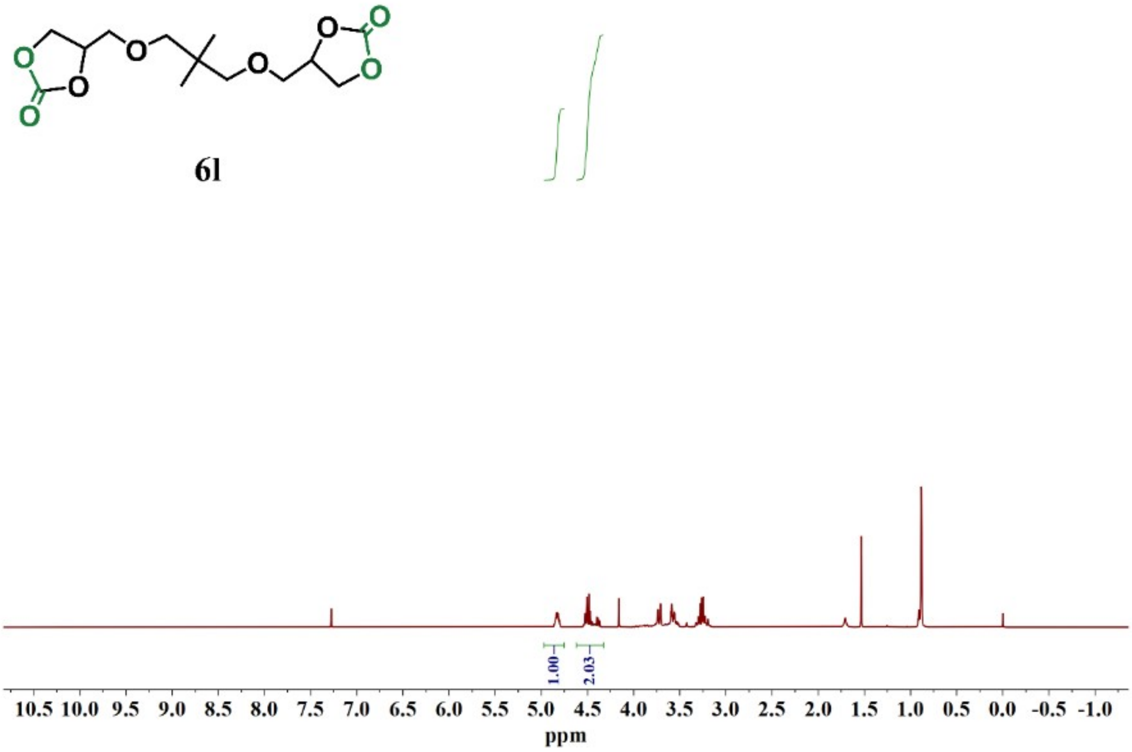

Fig. S52. ^{1}H NMR spectrum of **6l** (400 MHz, $CDCl_3$, 298 K).

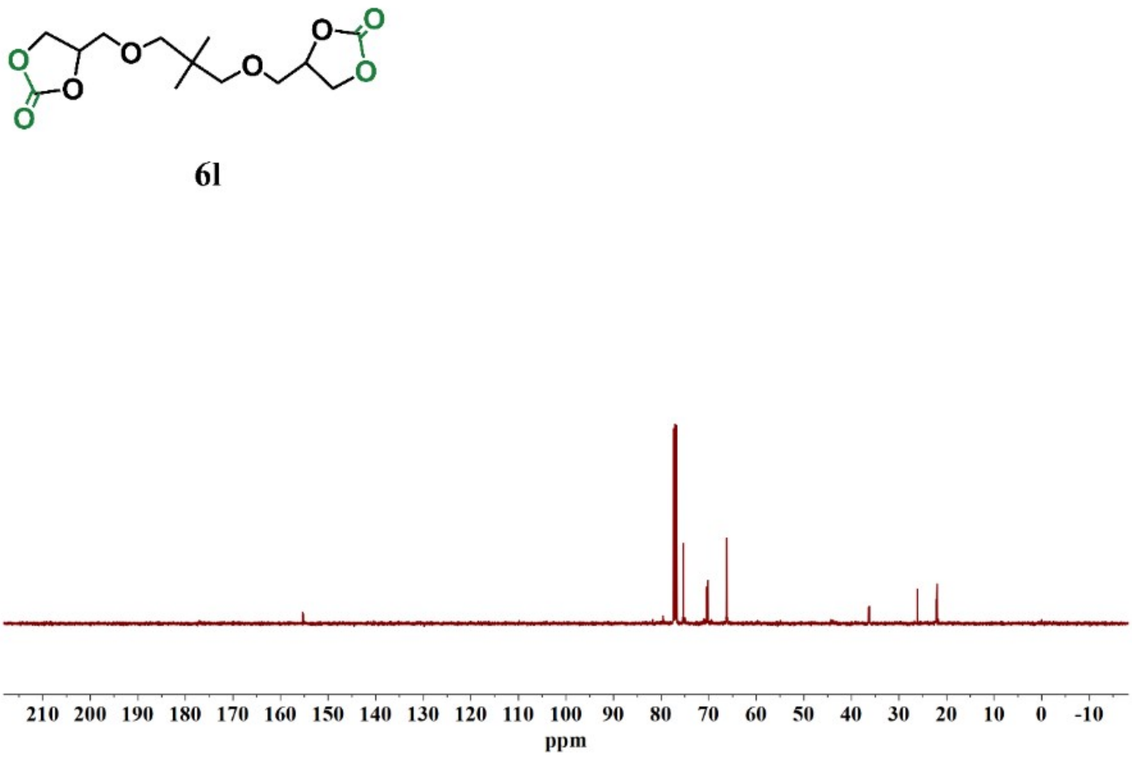

Fig. S53. ^{13}C NMR spectrum of **6l** (126 MHz, $CDCl_3$, 298 K).

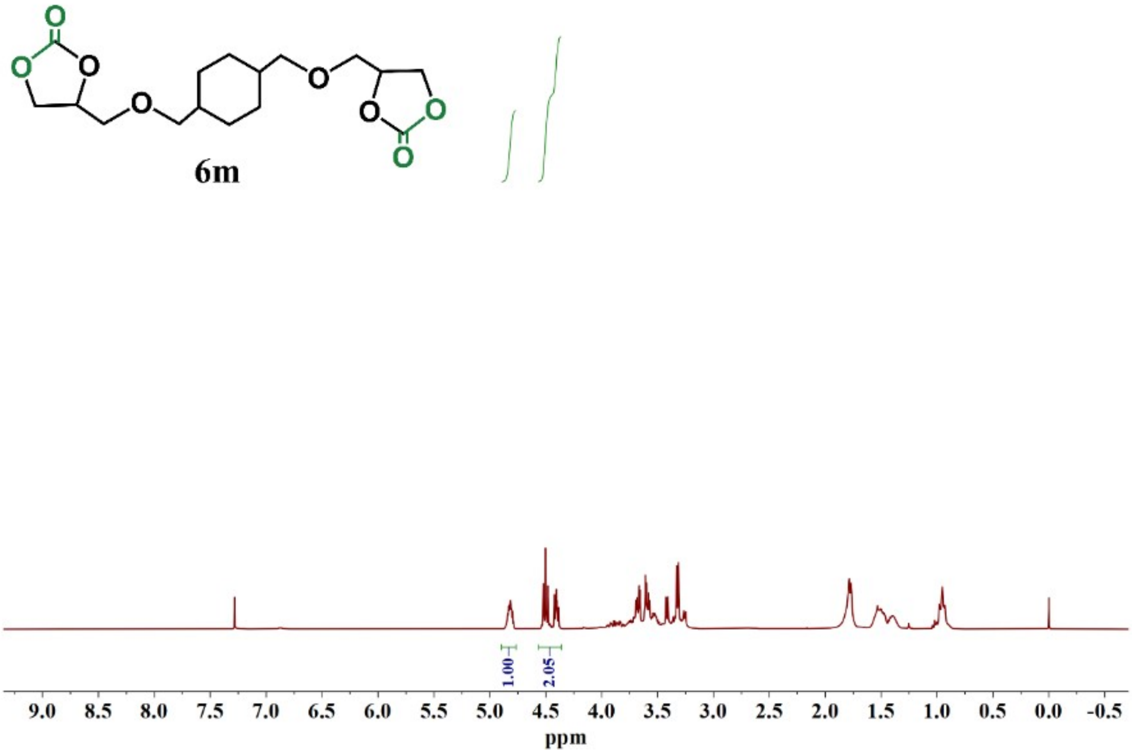

Fig. S54. ^{1}H NMR spectrum of **6m** (400 MHz, $CDCl_3$, 298 K).

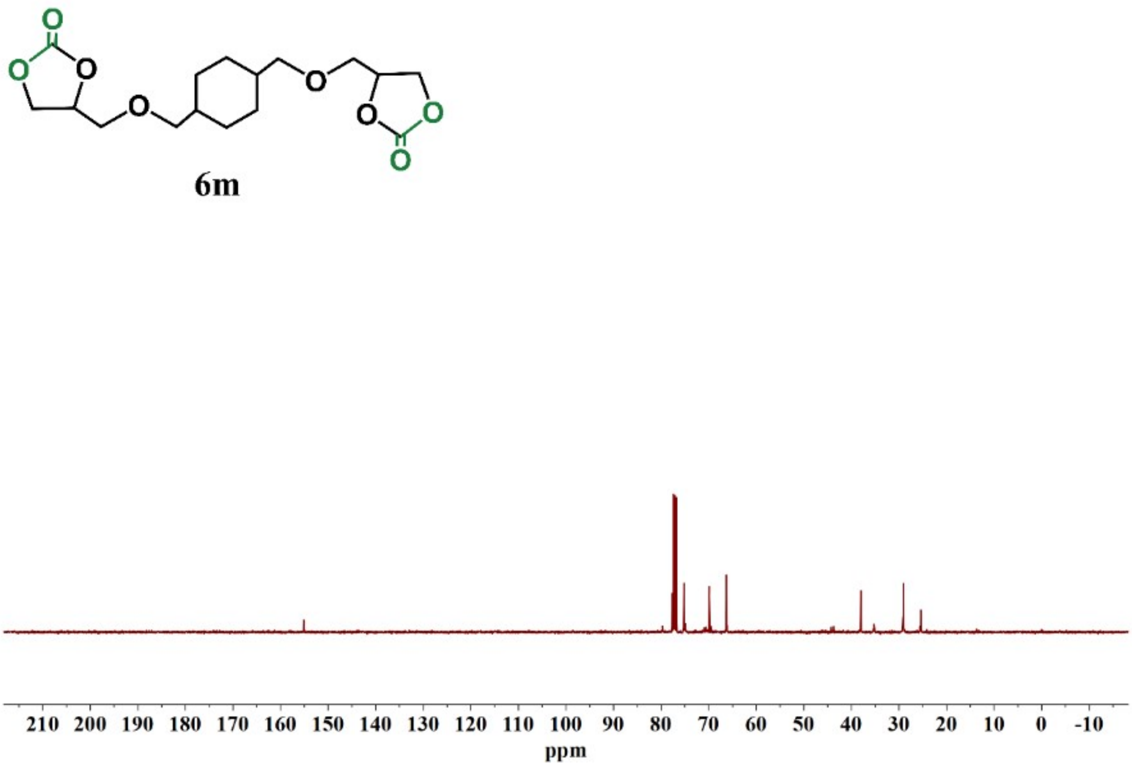

Fig. S55. ^{13}C NMR spectrum of **6m** (126 MHz, $CDCl_3$, 298 K).

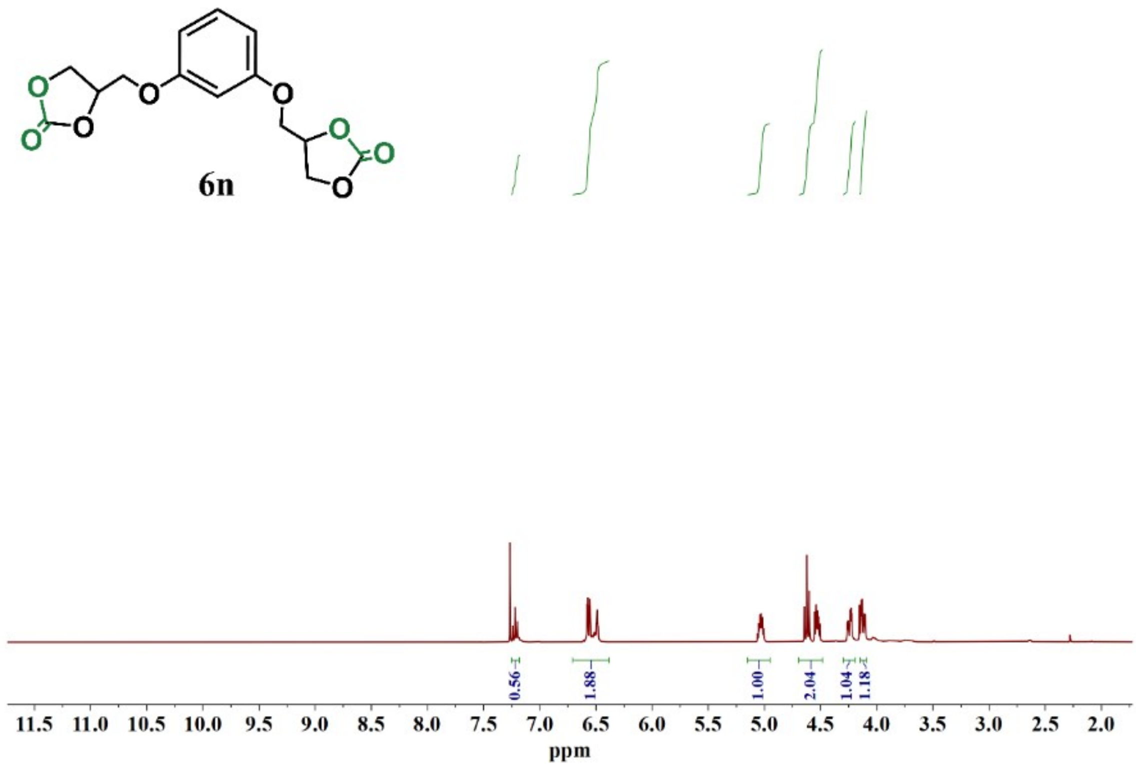

Fig. S56. ^{1}H NMR spectrum of **6n** (400 MHz, $CDCl_3$, 298 K).

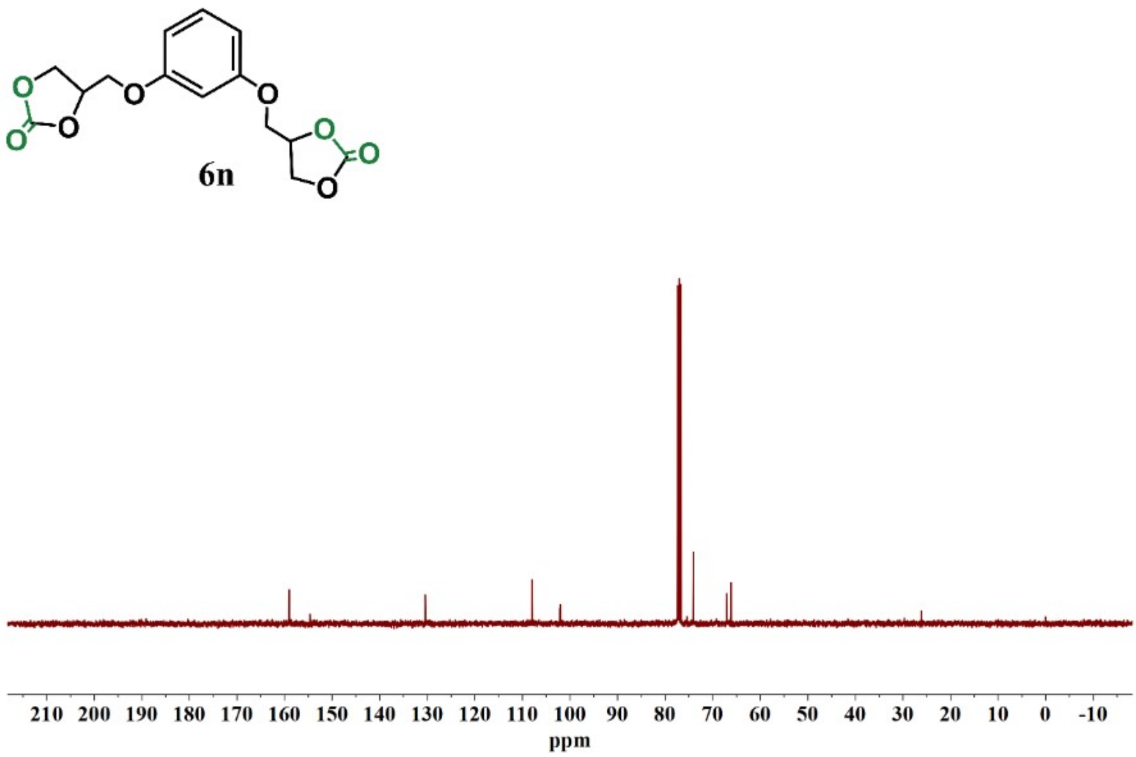

Fig. S57. ^{13}C NMR spectrum of **6n** (126 MHz, $CDCl_3$, 298 K).

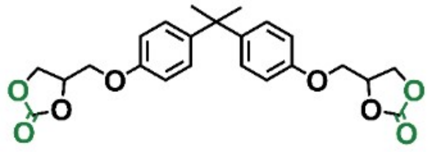

6o

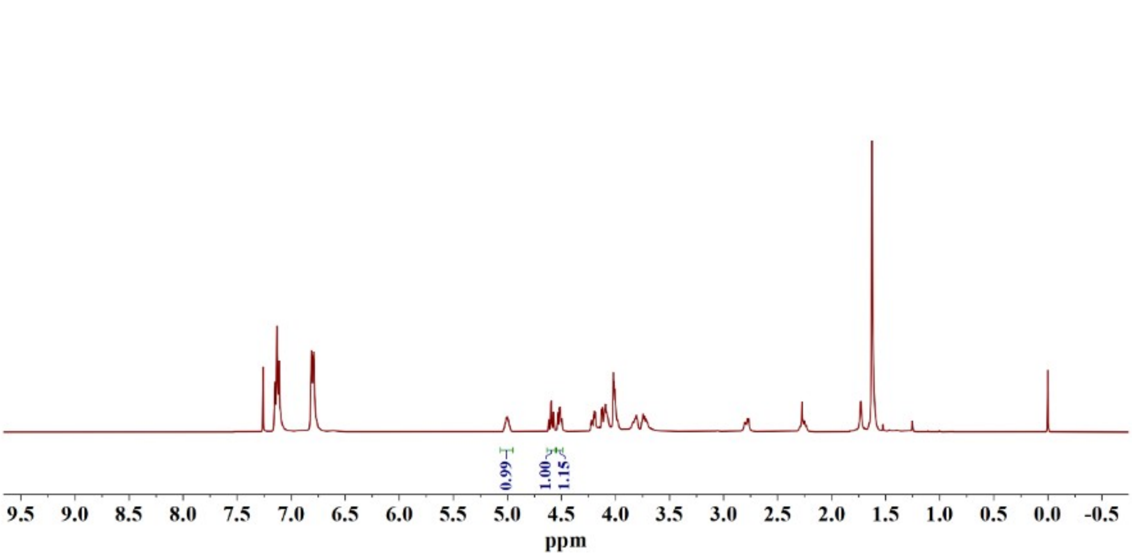

Fig. S58. ^{1}H NMR spectrum of **6o** (400 MHz, $CDCl_3$, 298 K).

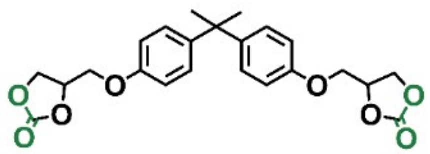

6o

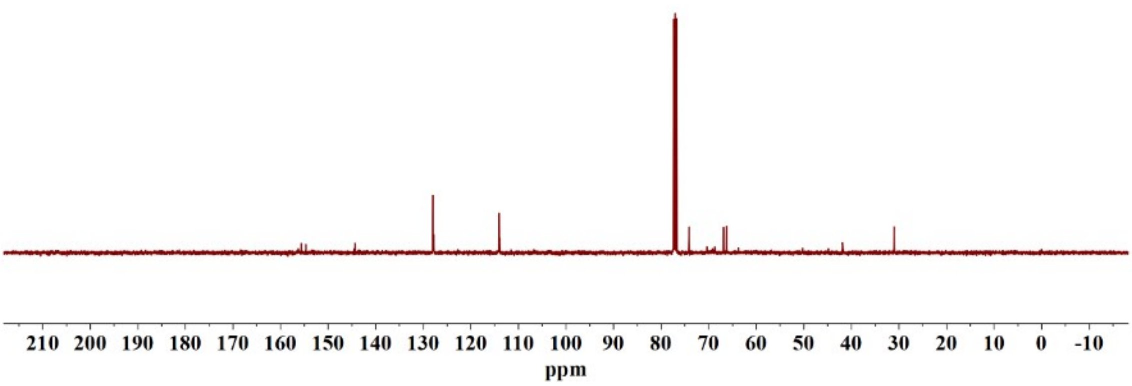

Fig. S59. ^{13}C NMR spectrum of **6o** (126 MHz, $CDCl_3$, 298 K).

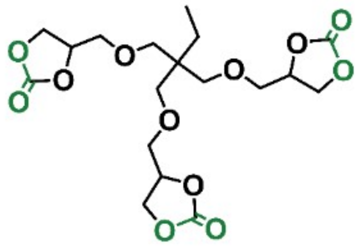

6p

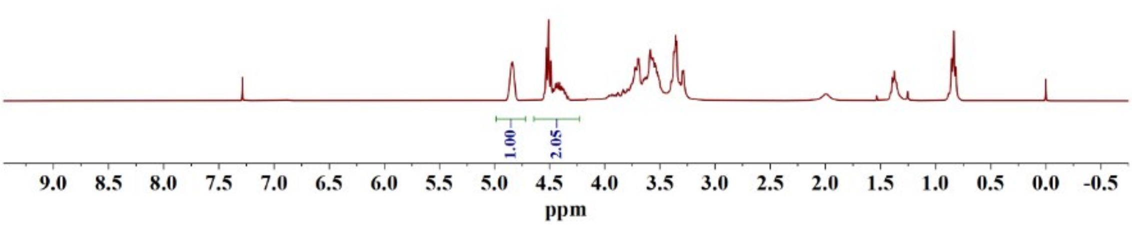

Fig. S60. ¹H NMR spectrum of **6p** (400 MHz, $CDCl_3$, 298 K).

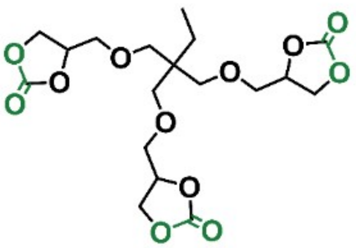

6p

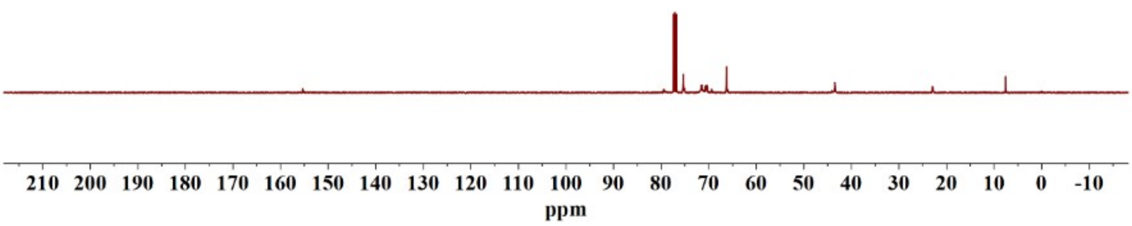

Fig. S61. ¹³C NMR spectrum of **6p** (126 MHz, $CDCl_3$, 298 K).

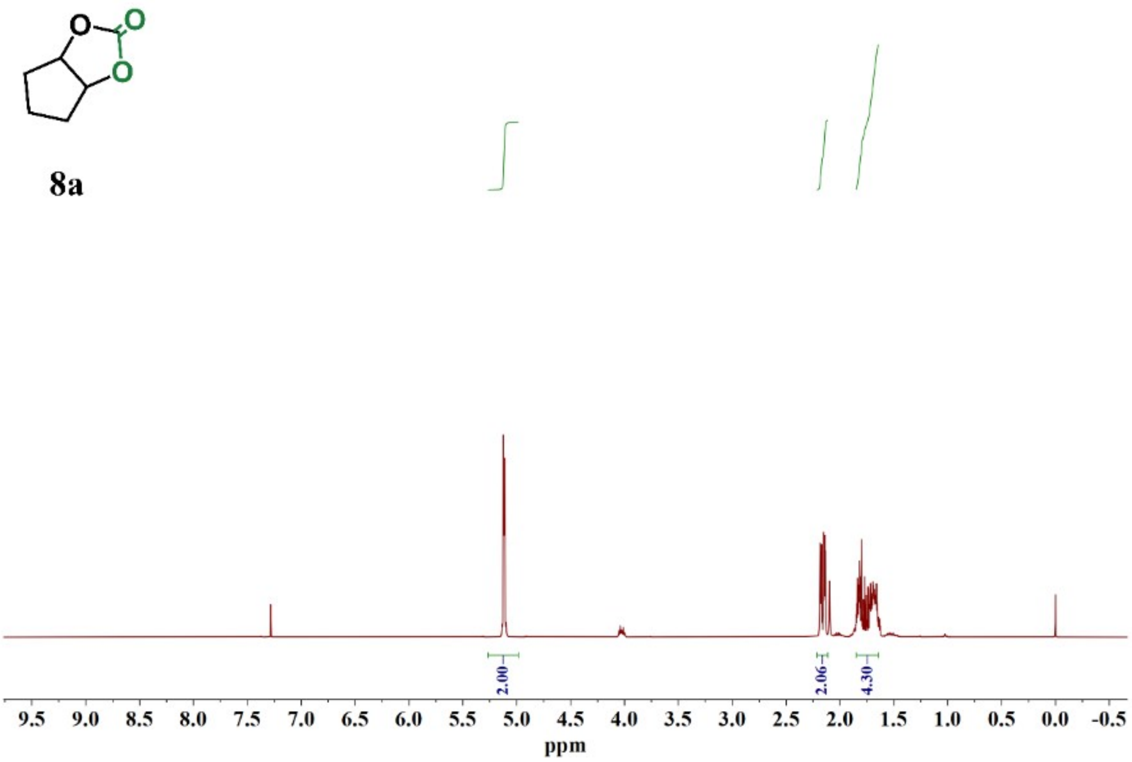

Fig. S62. ^{1}H NMR spectrum of **8a** (400 MHz, $CDCl_3$, 298 K).

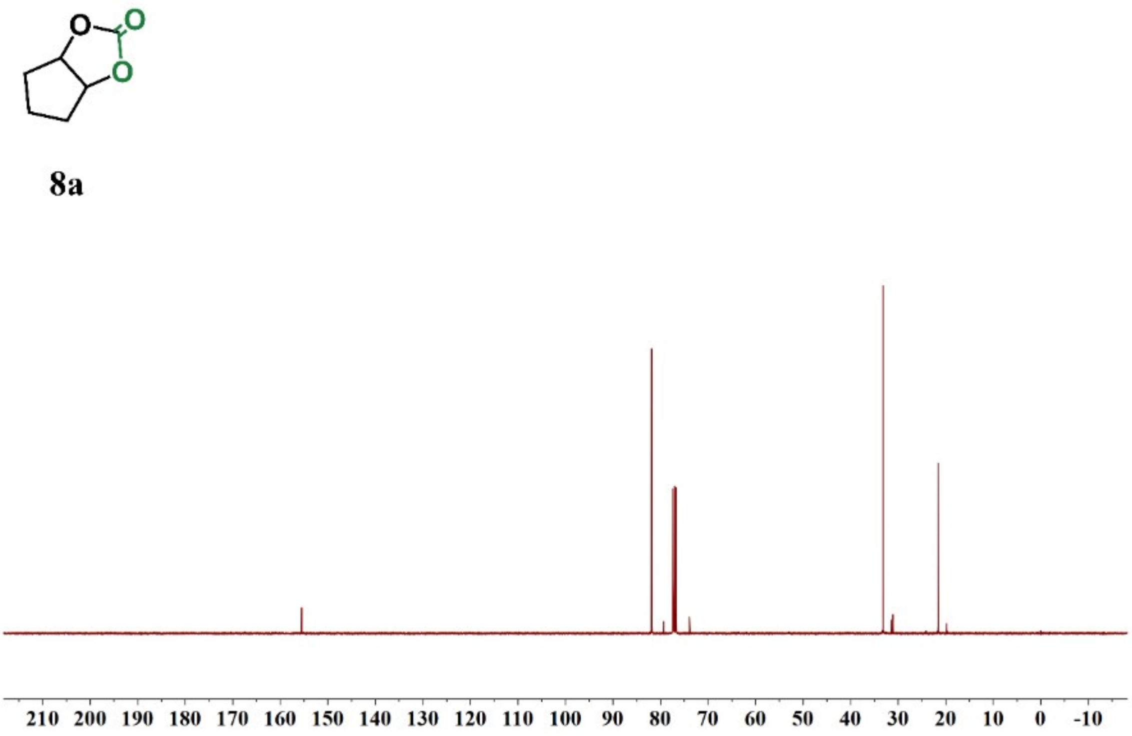

Fig. S63. ^{13}C NMR spectrum of **8a** (126 MHz, $CDCl_3$, 298 K).

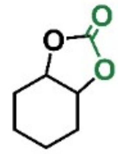

8b

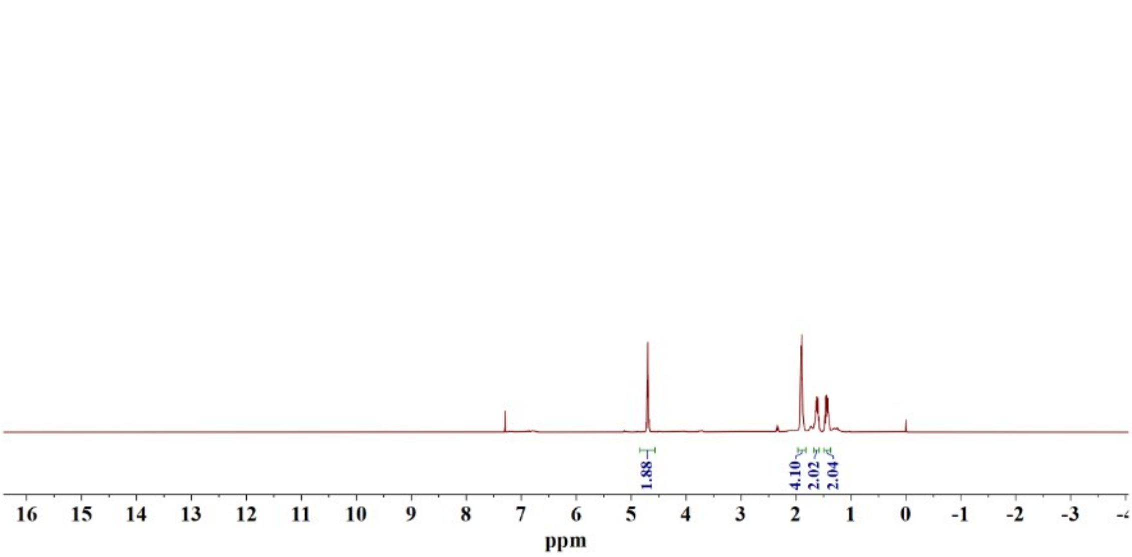

Fig. S64. ^{1}H NMR spectrum of **8b** (400 MHz, $CDCl_3$, 298 K).

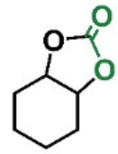

8b

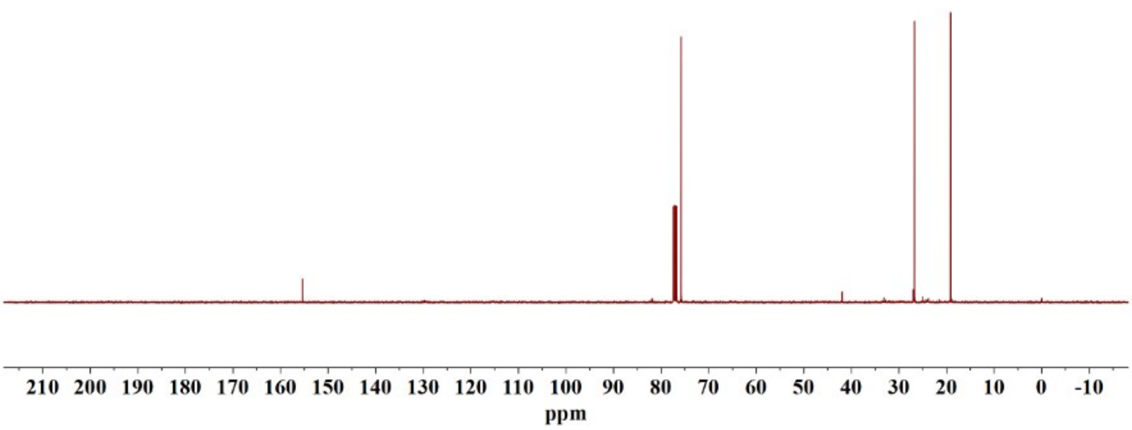

Fig. S65. ^{13}C NMR spectrum of **8b** (126 MHz, $CDCl_3$, 298 K).

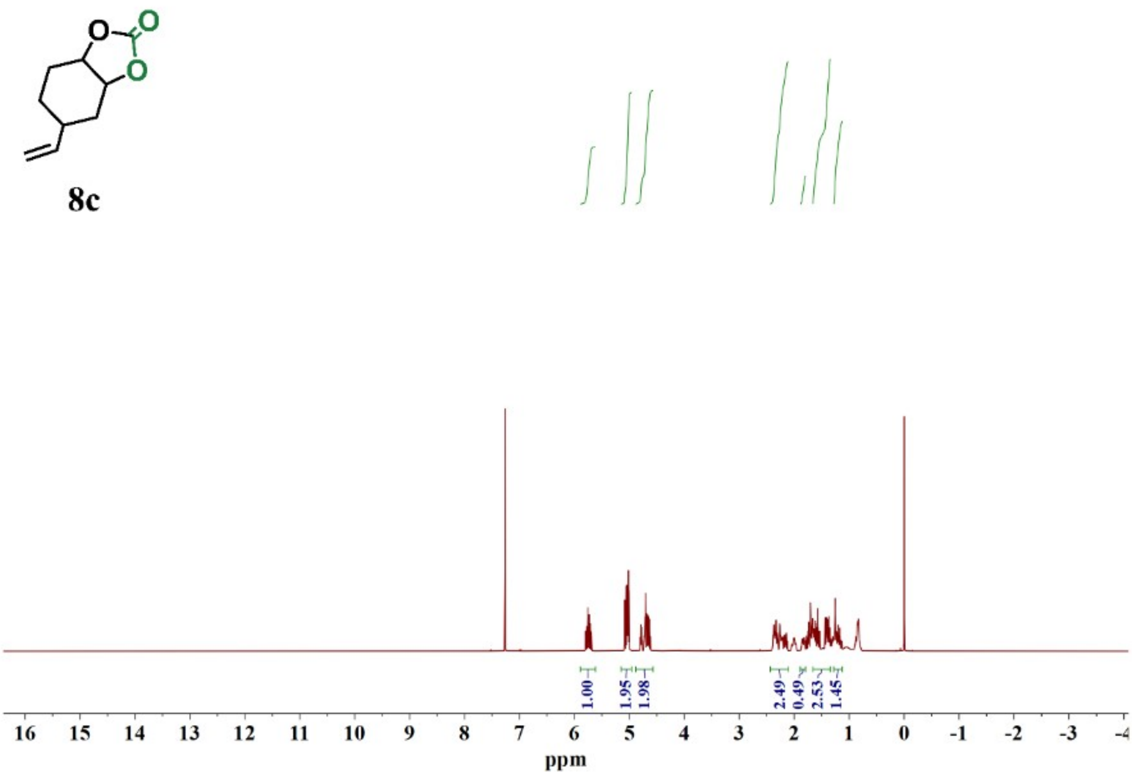

Fig. S66. ^{1}H NMR spectrum of **8c** (400 MHz, $CDCl_3$, 298 K).

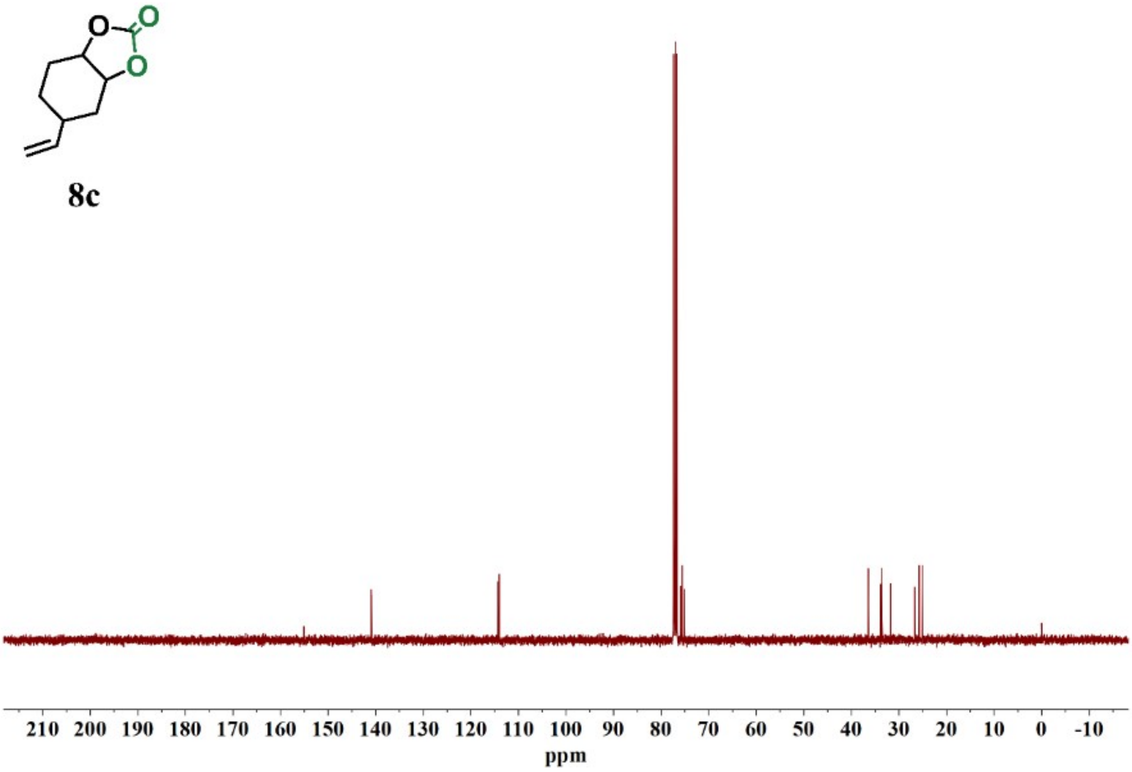

Fig. S67. ^{13}C NMR spectrum of **8c** (126 MHz, $CDCl_3$, 298 K).

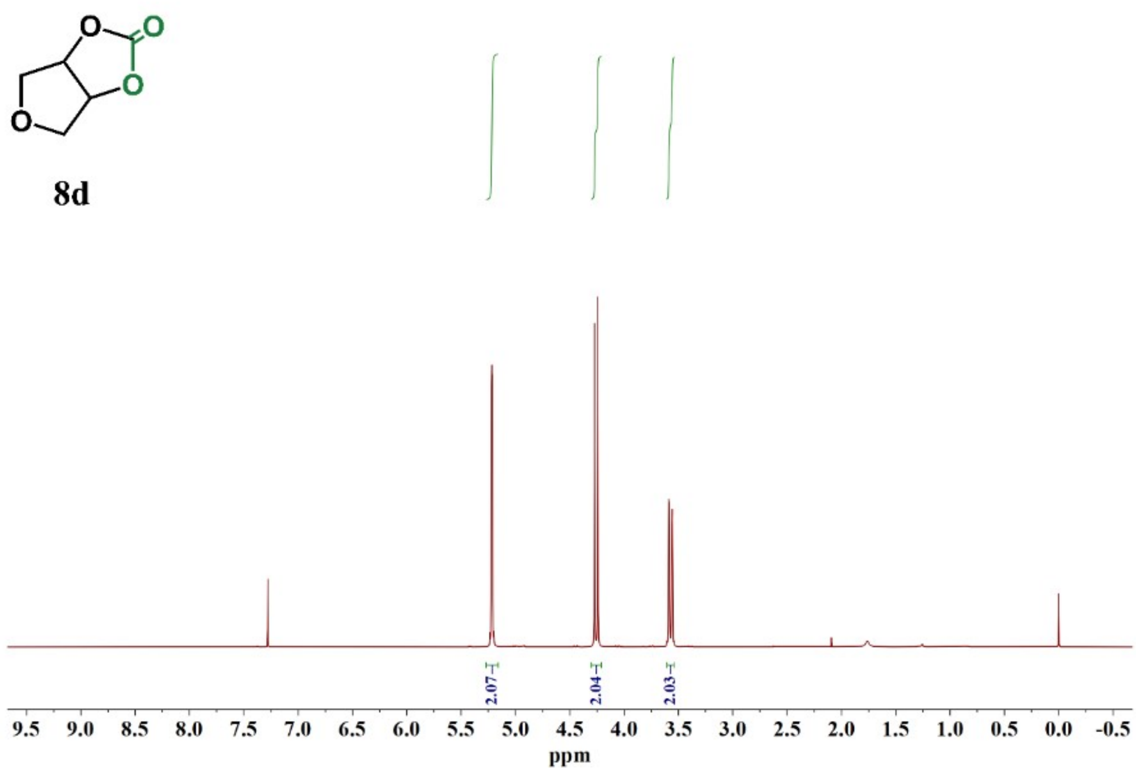

Fig. S68. ^{1}H NMR spectrum of **8d** (400 MHz, $CDCl_3$, 298 K).

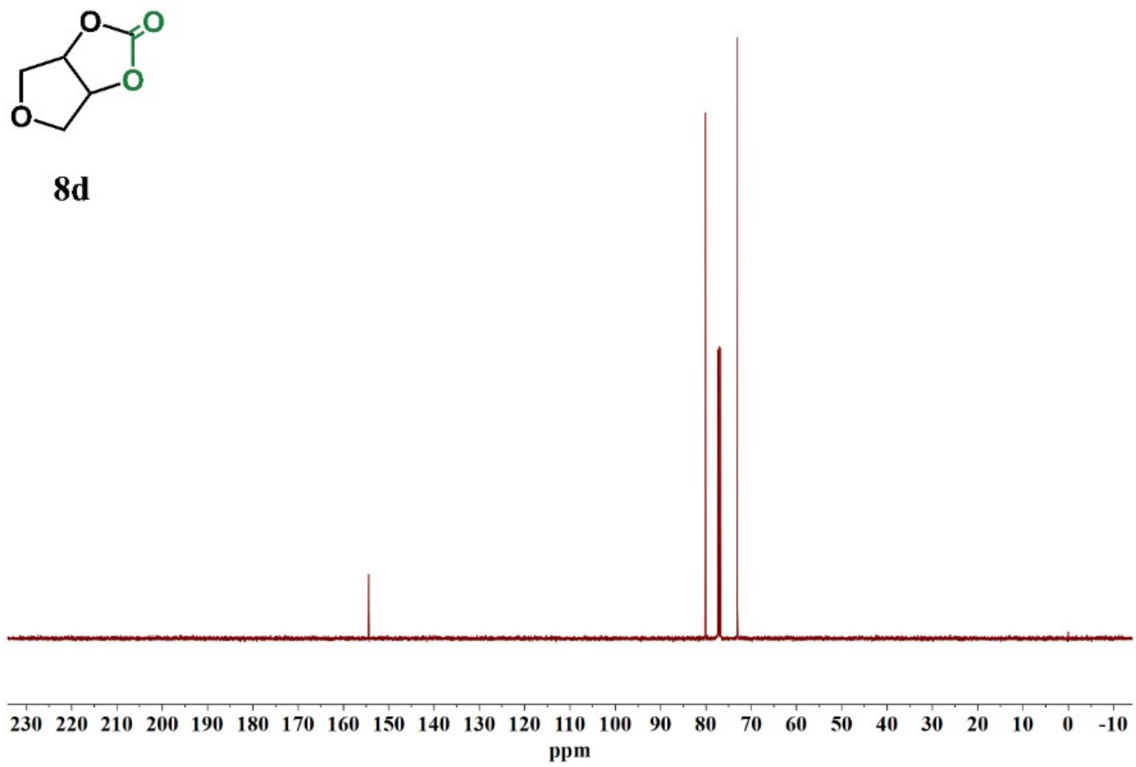

Fig. S69. ^{13}C NMR spectrum of **8d** (126 MHz, $CDCl_3$, 298 K).

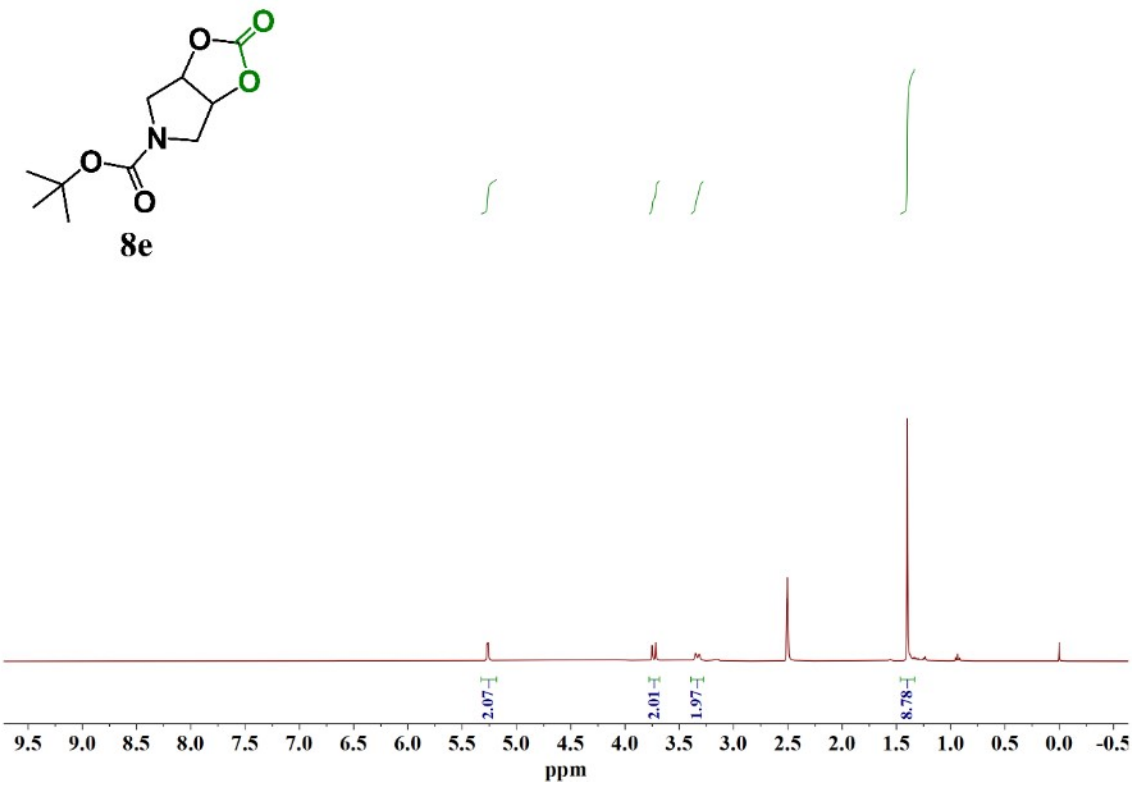

Fig. S70. ^{1}H NMR spectrum of **8e** (400 MHz, $CDCl_3$, 298 K).

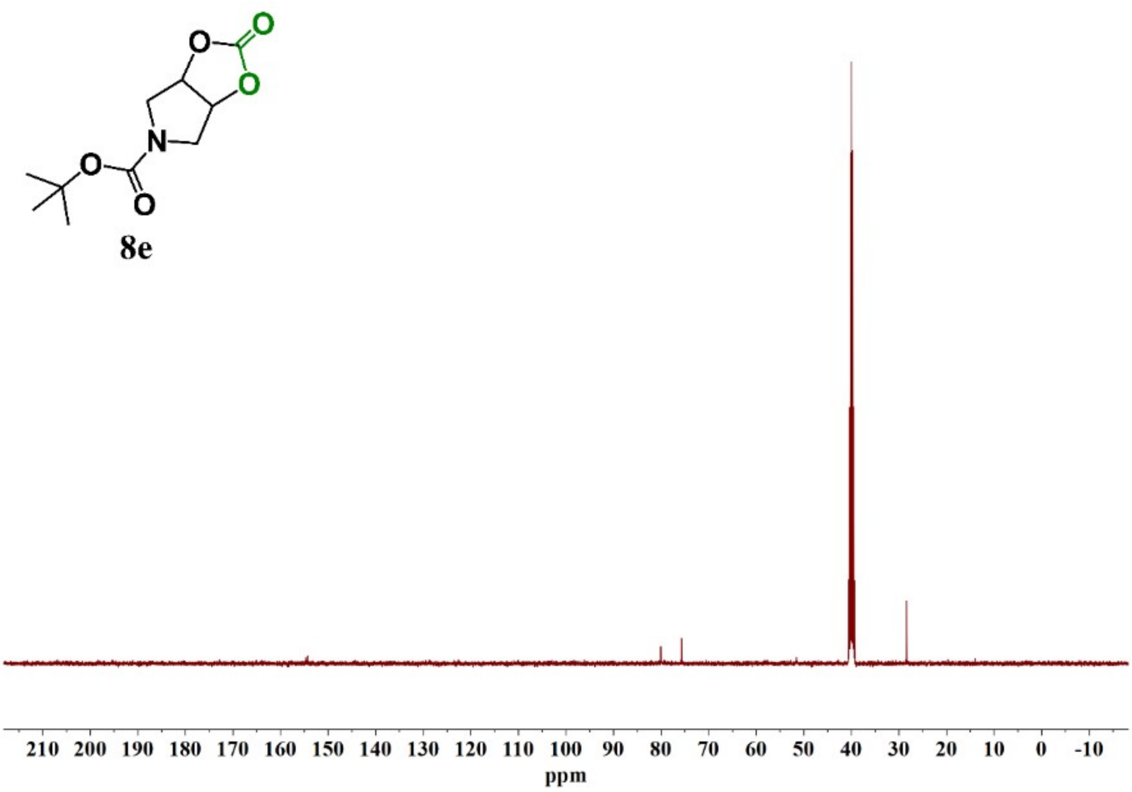

Fig. S71. ^{13}C NMR spectrum of **8e** (126 MHz, $CDCl_3$, 298 K).

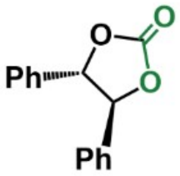

8f

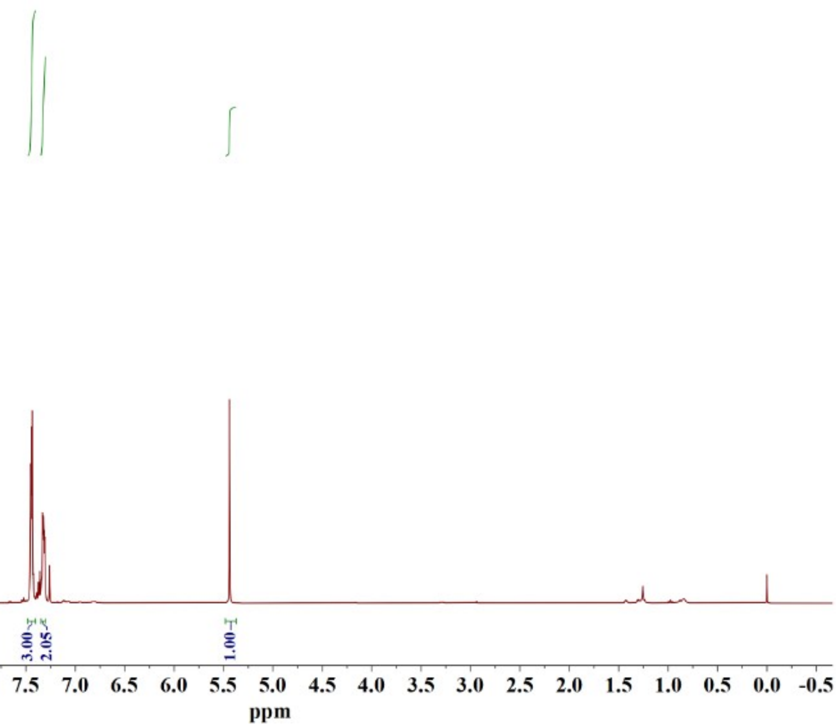

Fig. S72. ^{1}H NMR spectrum of **8f** (400 MHz, $CDCl_3$, 298 K).

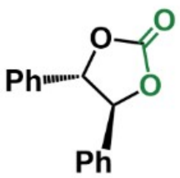

8f

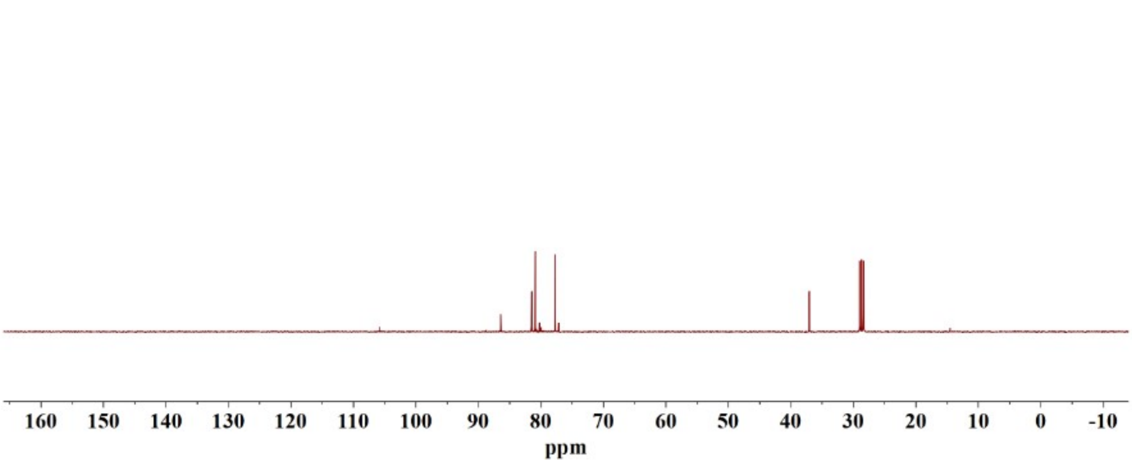

Fig. S73. ^{13}C NMR spectrum of **8f** (126 MHz, $CDCl_3$, 298 K).